Atlantic Hurricane Season of 2006

JAMES L. FRANKLIN AND DANIEL P. BROWN

National Hurricane Center, NOAA/NWS, Miami, Florida

(Manuscript received 11 September 2007, in final form 5 December 2007)

ABSTRACT

The 2006 Atlantic hurricane season is summarized and the year's tropical cyclones are described. A verification of National Hurricane Center official forecasts during 2006 is also presented. Ten cyclones attained tropical storm intensity in 2006. Of these, five became hurricanes and two became "major" hurricanes. Overall activity was near the long-term mean, but below the active levels of recent seasons. For the first time since 2001, no hurricanes made landfall in the United States. Elsewhere in the basin, hurricane-force winds were experienced in Bermuda (from Florence) and in the Azores (from Gordon). Official track forecast errors were smaller in 2006 than during the previous 5-yr period (by roughly 15%–20% out to 72 h), establishing new all-time lows at forecast projections through 72 h. Since 1990, 24–72-h official track forecast errors have been reduced by roughly 50%.

1. Introduction

Overall activity during the 2006 Atlantic season (Fig. 1; Table 1) was near average. There were ten tropical storms, of which five became hurricanes and two became major hurricanes [maximum 1-min winds of greater than 96 kt (1 kt = 0.5144 m s^{-1}), corresponding to category 3 or greater on the Saffir–Simpson Hurricane Scale (Saffir 1973; Simpson 1974)]. These numbers are very close to the 40-yr (1966–2005) averages of 11.1, 6.2, and 2.3, respectively, but represent activity considerably below that of recent seasons. Hurricane activity was relatively compressed, occurring only during a 37-day period between 27 August and 2 October. The last tropical cyclone activity of any kind also occurred on 2 October. Since the beginning of the geostationary satellite era (1966), only the 1983 and 1993 seasons have ended earlier (both on 30 September). In terms of "accumulated cyclone energy" [ACE; the sum of the squares of the maximum wind speed at 6-h intervals for (sub)tropical storms and hurricanes], activity this year was 90% of the long-term (1966–2005) mean, and the lowest observed since the 2002 season.

The near-average activity observed in 2006 appears to have resulted from two opposing factors. Atlantic waters were extremely warm in 2006; indeed, sea surface temperatures (SSTs) in the tropical Atlantic Ocean and Caribbean Sea between 10° and 20°N during the peak of hurricane season were the second highest since 1871 (only 2005 was warmer). While these warm SSTs and other atmospheric factors (e.g., relatively low shear) were conducive to an active hurricane season, the unexpected development of an El Niño event during the late summer appeared to suppress activity. Although the El Niño did not strongly affect the vertical wind shear throughout the basin, it likely caused or reinforced a strong area of anomalous subsidence over the western part of the Atlantic basin (Fig. 2). This sinking led to a warmer, drier, and more stable atmosphere that likely limited tropical cyclogenesis in this area (Bell et al. 2007).

For the first time since the 2001 season, and after twelve hurricanes struck the United States during 2004–2005,[1] none did so in 2006. Three tropical storms (Alberto, Beryl, and Ernesto) made landfall in the United States, although only Ernesto had a significant impact,

Corresponding author address: James L. Franklin, National Hurricane Center, NOAA/NWS, 11691 SW 17th Street, Miami, FL 33165-2149.
E-mail: james.franklin@noaa.gov

[1] This total includes Alex and Ophelia, which brought hurricane-force winds to the coastline but whose centers remained offshore.

DOI: 10.1175/2007MWR2377.1

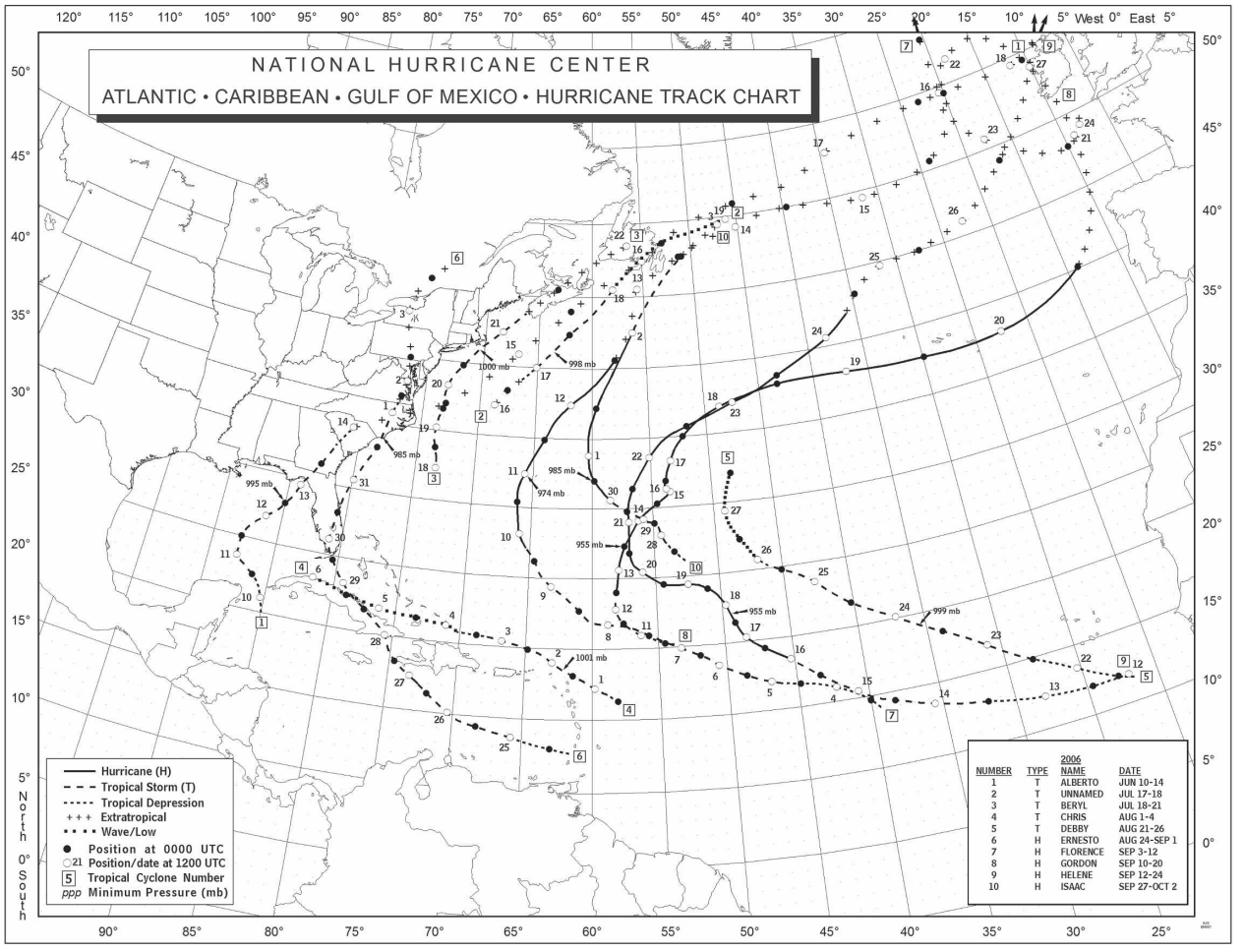

FIG. 1. Tracks of tropical storms and hurricanes in the Atlantic basin in 2006.

with damage estimated to have been near $500 million. No tropical cyclone–related direct deaths occurred in the United States during 2006. More significant impacts, however, were felt elsewhere in the basin. Alberto affected western Cuba, and Ernesto produced heavy rainfall in portions of Cuba, Haiti, and the Dominican Republic, with five deaths resulting from Ernesto's rains in Haiti. Florence brought hurricane

TABLE 1. 2006 Atlantic hurricane season statistics.

No.	Name	Class[a]	Dates[b]	Max 1-min wind (kt)	Min sea level pressure (mb)	Direct deaths	U.S. damage ($ million)
1	Alberto	T	10–14 Jun	60	995	0	Minor[c]
2	Unnamed	T	17–18 Jul	45	998	0	0
3	Beryl	T	18–21 Jul	50	1000	0	Minor[c]
4	Chris	T	1–4 Aug	55	1001	0	0
5	Debby	T	21–26 Aug	45	999	0	0
6	Ernesto	H	24 Aug–1 Sep	65	985	5	500
7	Florence	H	3–12 Sep	80	974	0	0
8	Gordon	H	10–20 Sep	105	955	0	0
9	Helene	H	12–24 Sep	105	955	0	0
10	Isaac	H	27 Sep–2 Oct	75	985	0	0

[a] T: tropical storm, wind speed 34–63 kt (17–32 m s^{-1}); H: hurricane, wind speed 64 kt (33 m s^{-1}) or higher.
[b] Dates begin at 0000 UTC and include tropical and subtropical depression stages but exclude extratropical stage.
[c] Only minor damage was reported, but the extent of the damage was not quantified.

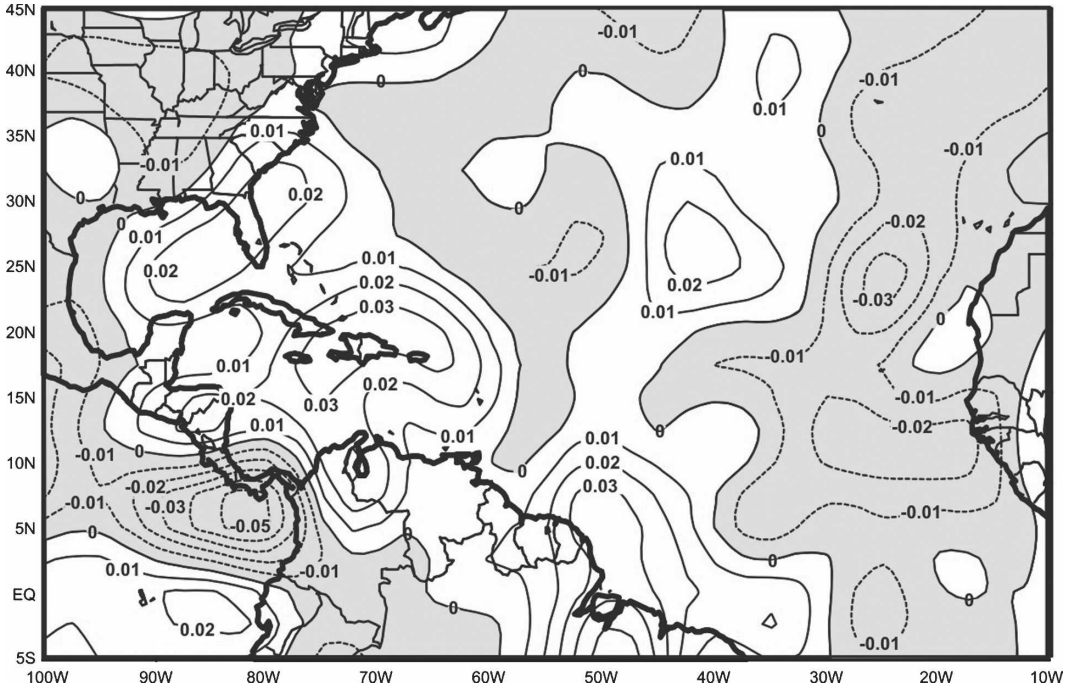

FIG. 2. Anomaly from the long-term (1968–96) mean of vertical velocity (Pa s^{-1}) for August–October 2006. Areas of anomalous rising motion are shaded. [Data provided by the NOAA/Cooperative Institute for Research in Environmental Sciences Climate Diagnostics Center, Boulder, CO (http://www.cdc.noaa.gov/), based on the National Centers for Environmental Prediction–National Center for Atmospheric Research reanalysis project (Kistler et al. 2001).]

conditions to Bermuda, and after losing tropical characteristics also brought hurricane-force winds to portions of Newfoundland. Gordon was the first hurricane to affect the Azores since 1991.

The lack of hurricane landfalls on the North American continent in 2006 is attributed to large-scale steering patterns that were markedly different from those present during 2004 and 2005 (Fig. 3). September 2006 was characterized by a strong midlevel trough over the eastern United States, a pattern conducive to steering the four hurricanes that formed during the month out to sea, near or east of Bermuda. This pattern was reminiscent of the dominant steering flow that prevailed during 1995–2003. In contrast, the mean September steering patterns for 2004 and 2005 featured high pressure over the western Atlantic and eastern United States that kept many systems on more westward tracks.

2. Storm and hurricane summaries

The individual cyclone summaries that follow are based on National Hurricane Center (NHC) poststorm meteorological analyses of a wide variety of (often contradictory) data described below. These analyses result in the creation of a "best-track" database for each storm, consisting of 6-hourly representative estimates of the cyclone's center position, maximum sustained (1-min average) surface (10 m) wind, minimum sea level pressure, and maximum extent of 34-, 50-, and 64-kt winds in each of four quadrants around the center. The tracks and basic statistics for the season's storms and hurricanes are given in Fig. 1 and Table 1, respectively (also see online at http://www.nhc.noaa.gov/pastall.shtml).[2] The life cycle of each cyclone (as indicated by the dates given in Table 1) is defined to include the tropical or subtropical depression stage, but does not include remnant low or extratropical stages.

For storms east of 55°W, or those not threatening land, the primary (and sometimes sole) source of information is geostationary weather satellite imagery, interpreted using the Dvorak (1984) or Hebert–Poteat (Hebert and Poteat 1975) techniques. Ships and buoys occasionally provide important in situ observations on

[2] Tabulations of the 6-hourly best-track positions and intensities can be found in the NHC tropical cyclone reports (see Web address in text). These reports contain storm information omitted here because of limitations of space, including additional surface observations and a forecast and warning critique.

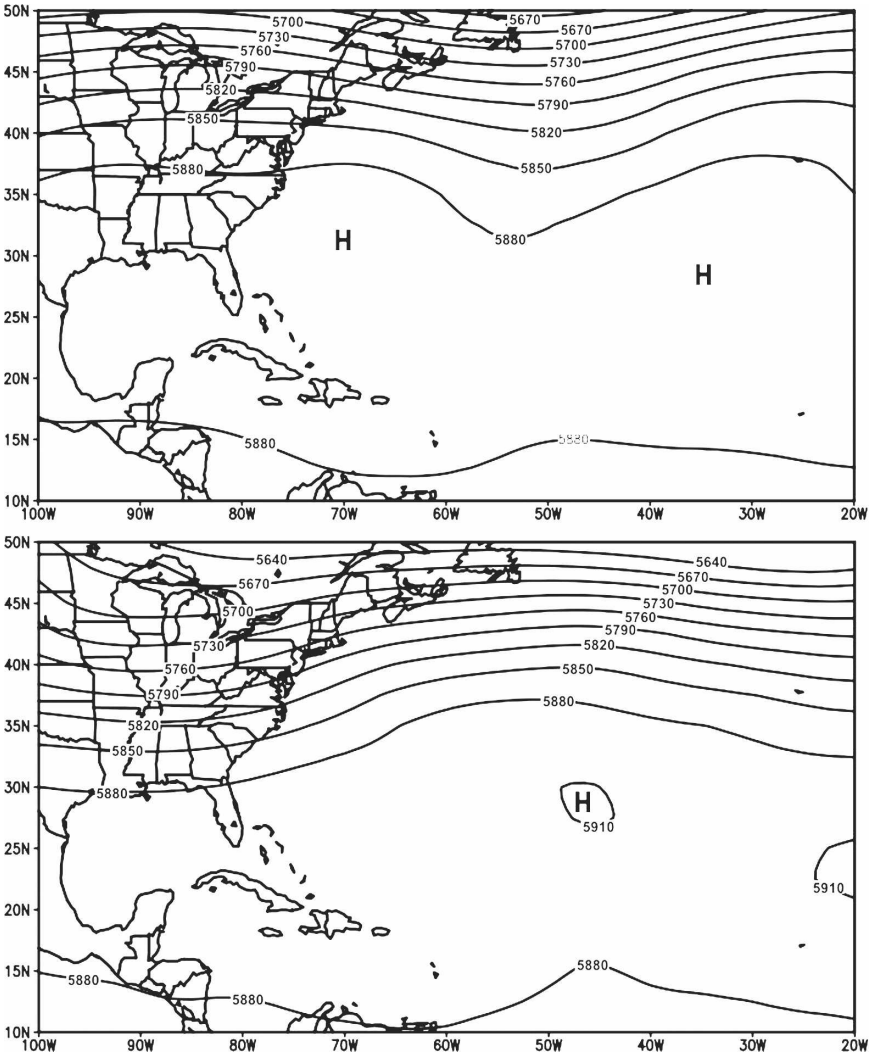

FIG. 3. Mean 500-mb heights (m) for September (top) 2004–05 and (bottom) 2006. Source of data same as in Fig. 2.

these cyclones. For systems posing a threat to land, in situ observations are also generally available from aircraft reconnaissance flights conducted by the 53rd Weather Reconnaissance Squadron ("Hurricane Hunters") of the Air Force Reserve Command (AFRC), and by the National Oceanic and Atmospheric Administration (NOAA) Aircraft Operations Center (AOC). During reconnaissance flights, minimum sea level pressures are either measured by dropsondes released at the circulation center or extrapolated hydrostatically from flight level. Low-level winds in the eyewall or maximum wind band are often measured directly using global positioning system (GPS) dropwindsondes (Hock and Franklin 1999), but more frequently are estimated from flight-level winds using empirical relationships derived from a 3-yr sample of GPS dropwindsonde data (Franklin et al. 2003). During NOAA reconnaissance missions, surface winds can be estimated remotely using the Stepped-Frequency Microwave Radiometer (SFMR) instrument (Uhlhorn and Black 2003). For storms close to land, weather radars, buoys, and conventional land-based surface and upper-air observations supplement the satellite and reconnaissance data. In key forecast situations, the kinematic and thermodynamic structure of the storm environment is obtained from dropsondes released during operational "synoptic surveillance" flights of NOAA's Gulfstream IV jet aircraft (Aberson and Franklin 1999).

Several satellite-based technologies play an important role in the analysis of tropical weather systems. Foremost of these is multichannel passive microwave imagery [e.g., from the Tropical Rainfall Measuring

Mission (TRMM) satellite], which over the past decade has provided radarlike depictions of systems' convective structure (Hawkins et al. 2001) and is of great help in assessing system location and organization. The SeaWinds scatterometer onboard the Quick Scatterometer (QuikSCAT) satellite (Tsai et al. 2000) provides surface winds over large oceanic swaths. While the QuikSCAT generally does not have the horizontal resolution to determine a hurricane's maximum winds, it can often be used to estimate the intensity of weaker systems and to determine the extent of tropical storm–force winds. In addition, it can be helpful in resolving whether an incipient tropical cyclone has acquired a closed surface circulation. Finally, information on the thermal structure of cyclone cores is provided by the Advanced Microwave Sounder Unit (AMSU; Velden and Brueske 1999). Intensity estimates derived from such data in some cases can be superior to Dvorak classifications (Herndon and Velden 2004).

A number of organizations have developed Web sites that have proven to be extremely helpful for tropical cyclone forecasting and postanalysis. These sites include the Naval Research Laboratory (NRL) Monterey Marine Meteorology Division Tropical Cyclone Page (http://www.nrlmry.navy.mil/tc_pages/tc_home.html), with its comprehensive suite of microwave products, the cyclone phase diagnostics page of the Florida State University (http://moe.met.fsu.edu/cyclonephase/), which is frequently consulted to help categorize systems as tropical, subtropical, or nontropical, and the tropical cyclone page of the University of Wisconsin—Madison Cooperative Institute for Meteorological Satellite Studies (http://cimss.ssec.wisc.edu/tropic/tropic.html), which contains a variety of useful satellite-based synoptic analyses.

In the cyclone summaries below, U.S. property damage estimates have been generally estimated by doubling the insured losses reported by the Property Claim Services of the Insurance Services Office. The reader is cautioned, however, that great uncertainty exists in determining the cost of the damage caused by tropical cyclones when they make landfall. Descriptions of the type and scope of damage are taken from a variety of sources, including local government officials, media reports, and local National Weather Service (NWS) Weather Forecast Offices (WFOs) in the affected areas. Tornado counts are based on reports provided by the WFOs and/or the Storm Prediction Center. Hard copies of these various reports are archived at the NHC.

Although specific dates and times in these summaries are given in coordinated universal time (UTC), local time is implied whenever general expressions such as "afternoon," "midday," etc. are used.

a. Tropical Storm Alberto, 10–14 June

Alberto formed from an area of disturbed weather that persisted for several days over Central America and the northwestern Caribbean Sea. Convection in the area increased on 8 June with the arrival of a westward-moving tropical wave, and pressures began to fall between the Yucatan Peninsula and Cuba where the convection was most concentrated. By 0600 UTC 10 June, the disturbance had acquired a surface circulation and sufficiently organized convection to be classified as a tropical depression. The depression, initially centered about 120 n mi south of the western tip of Cuba, moved slowly northwestward, becoming a tropical storm at 0000 UTC 11 June about 60 n mi northeast of the northeastern tip of the Yucatan Peninsula. Strong southwesterly shear in the Gulf of Mexico kept the main area of convection displaced from the circulation center, and there was little change in Alberto's strength until the following day. As the storm interacted with the deep warm waters of the Loop Current early on 12 June, convection increased. By late morning, a circulation center had reformed near the convection about 60 n mi to the northeast of its previous position (Fig. 4), and Alberto's maximum winds increased abruptly to 60 kt. The system's minimum pressure of 995 mb was reached a few hours later, near 0000 UTC 13 June, when Alberto was centered about 100 n mi south of Apalachicola, Florida.

Alberto's increase in organization was short lived. While the cyclone moved northeastward in the eastern Gulf of Mexico, its cloud pattern became elongated and the convection began to diminish. Dry air overtook the cyclone early on 13 June and Alberto began to weaken as it moved toward Florida's Big Bend region. Alberto made landfall near Adams Beach at about 1630 UTC 13 June with maximum winds of 40 kt. Alberto continued to weaken after it moved inland, becoming a depression early on 14 June and losing tropical characteristics later that day over South Carolina. The extratropical remnant of Alberto moved across North Carolina and into the Atlantic, where it became a powerful extratropical storm just south of Nova Scotia. The cyclone slowly weakened as it continued across the North Atlantic Ocean to the British Isles, where it was finally absorbed by a frontal system on 19 June.

The strongest wind reported in Alberto was a flight-level observation of 81 kt from a NOAA WP-3D aircraft, at an altitude of 5000 ft at 1657 UTC 12 June, although this observation was considered to represent a transient convective feature. Selected surface observa-

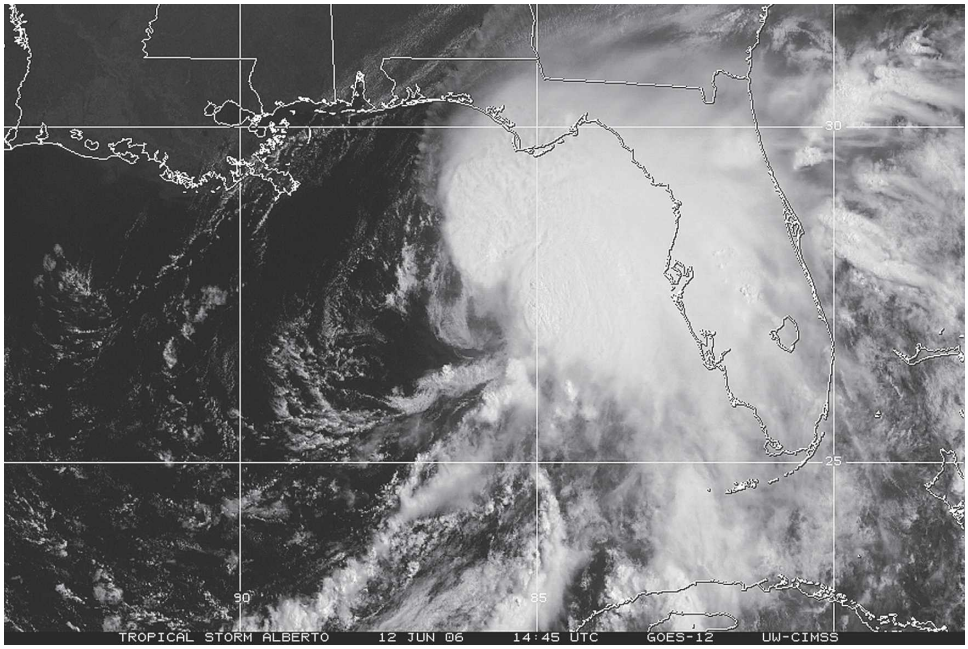

FIG. 4. *Geostationary Operational Environmental Satellite-12* (*GOES-12*) visible satellite image of Tropical Storm Alberto at 1445 UTC 12 Jun 2006, near the time of the cyclone's maximum intensity (image courtesy of University of Wisconsin—Madison).

tions from land stations and data buoys are given in Table 2. Alberto produced torrential rains in western Cuba, where there was one report of 445 mm and several others in excess of 300 mm. The highest reported rainfall in the United States was 179.8 mm near Tarpon Springs, Florida. There were several reports of sustained tropical storm–force winds in Florida, the highest of which (42 kt) occurred at the Old Port Tampa National Ocean Service (NOS) site. There were seven tornadoes in South Carolina, most of them rated as F0.

Property losses associated with Alberto were relatively minor. In Florida, storm surge flooding near Homossassa in Citrus County put 1 m of water into a restaurant and damaged 20 homes. Numerous houses suffered flood damage in Levy County, and a few downed trees in Tallahassee caused power outages. There were no "direct" deaths associated with Alberto as a tropical cyclone. After the system became extratropical, however, an 8-yr-old boy was pulled into a drainage system and drowned near Raleigh, North Carolina. There was also a press report of four sailors missing about 200 n mi south of Nova Scotia when Alberto passed by during its extratropical storm stage.

b. Unnamed tropical storm, 17–18 July

As part of its routine postseason review, NHC occasionally identifies a previously undesignated tropical or subtropical cyclone based on new data or meteorological interpretation. This year's review reclassified a short-lived system as a tropical storm.

The tropical cyclone originated along the tail end of a cold front that moved offshore of the northeastern United States late on 13 July and stalled over the western Atlantic Ocean. An extratropical low formed on 16 July along the decaying front when an upper trough approached from the west. The upper trough weakened, and the surface low moved slowly northeastward over warm 27°–28°C waters. Buoy and satellite data suggest that the front associated with the low dissipated late on 16 July, although the low lacked organized convection until early the next day, when a large burst of convection formed near the center. It is estimated that a tropical depression formed at 0600 UTC 17 July about 210 n mi southeast of Nantucket Island, Massachusetts.

Satellite intensity estimates indicate that the depression attained tropical storm strength 6 h later while accelerating toward the northeast. A large curved band of convection formed in the northern portion of the storm, with other banding features becoming more prominent throughout the day, and the system reached a peak intensity of about 45 kt near 1800 UTC 17 July. Shortly thereafter, the cyclone crossed the north wall of the Gulf Stream and encountered much cooler waters. Convection diminished significantly overnight, and by 1200 UTC 18 July the system became a nonconvective remnant low. The remnant low moved across New-

TABLE 2. Selected surface observations for Tropical Storm Alberto, 10–14 Jun.

Location	Min sea level pressure		Max surface wind speed			Storm surge (m)[c]	Storm tide (m)[d]	Tot rain (mm)
	Date/time (UTC)	Pressure (mb)	Date/time (UTC)[a]	Sustained (kt)[b]	Gust (kt)			
			Cuba					
Ciro Redondo, Pinar del Rio								304.0
Consolación del Sur, Pinar del Rio								323.1
Derivadota Jagua, Isla de la Juventud								301.0
Francia, Isla de la Juventud								335.0
Herradura, Pinar del Rio								286.0
Las Terrazas, Pinar del Rio								246.9
Minas de Matahambre, Pinar del Rio								265.9
Playa Baracoa, La Habana								214.9
Presa Mal Pais, Isla de la Juventud								309.9
Rio Seco, Pinar del Rio								445.0
Sabanilla, Pinar del Rio								309.9
San Juan y Martinez, Pinar del Rio								281.2
Santa Fe, Isla de la Juventud								253.0
Santa Lucia, Pinar del Rio								208.0
Sumidero, Pinar del Rio								398.0
			Florida					
Apalachicola (KAAF)	13/0956	1003.3	13/0556	24	31			45.5
Brooksville (KBKV)	13/0859	1006.8	13/1928	24	37			66.0
Clearwater Beach National Ocean Service (NOS) (CWBF1)	13/0800	1005.9	13/0354	40	52	0.7	1.2	
Daytona Beach (KDAB)	13/1052	1010.2	13/1614	26	32			91.7
Fernandina Beach NOS (FRDF1)			13/2348	28	38		1.7	
Fort Myers NOS (FMRF1)						0.5	0.6	
Fort Pierce (KFPR)			11/1753	29	40			
Jacksonville Craig Field (KCRG)	13/2053	1007.7	13/2253	27	40			
Jacksonville (KJAX)	13/2056	1006.9	13/1956	25	38			71.1
Jacksonville Cecil Field (KVQQ)	13/1950	1007.5	13/1950	20	47			
Jacksonville NAS (NIP)	13/2055	1007.3	13/2055	24	34			
Leesburg (KLEE)	13/1004	1008.1	11/1733	29	40			60.5
MacDill Air Force Base (AFB) (KMCF)	13/0434	1006.4	13/0637	33	49			86.1
Mayport Naval Air Station (NAS) (KNRB)	13/1855	1008.1	13/1802	22	36			57.9
Mayport NOS (MYPF1)	13/1912	1009.4	13/0812	27	39		1.5	
McKay Bay NOS (MCYF1)			13/0712	37	47	1.0	1.4	
Melbourne (KMLB)	13/0729	1010.5	11/1755	31	49			58.9
Ocala (KOCF)	13/0853	1007.1	13/1655	28	37			33.3
Old Port Tampa NOS (OPTF1)			13/0500	42	52	0.8	1.3	
Orlando (KMCO)	13/0724	1009.2	13/0724	33	46			72.6
Orlando (KORL)	13/0721	1009.8	13/1810	31	37			88.4
Perry (40J)	13/1735	997.2						111.5
Port Manatee NOS (PMAF1)			13/0730	29	38	0.6	1.0	
Punta Gorda (KPGD)	13/0724	1010.5	13/0729	28	40			58.9
Sanford (KSFB)	13/0803	1009.2	13/1534	31	46			102.4
Sarasota (KSRQ)	13/0908	1008.1	13/0640	29	38			114.6
St. Petersburg (KPIE)	13/0836	1007.1	13/0540	35	44			100.8
St. Petersburg (KSPG)	13/0810	1007.1	13/0637	32	42			81.3
St. Petersburg NOS (SAPF1)			13/0324	30	41	0.8	1.2	
Tallahassee (KTLH)	13/1118	1004.0	13/0550	30	33			82.6
Tampa (KTPA)	13/0931	1007.8	13/0509	29	39			87.9
Tampa Birth 223 NOS (ERTF1)			13/0730	34	40			
The Villages (KVVG)	13/0745	1008.1	13/1805	24	36			22.1
Titusville (KTTS)	13/0855	1010.5	13/1809	26	44			
Vandenburg (KVDF)	13/2050	1007.5	13/1801	26	47			
Vero Beach (KVRB)	13/0817	1010.8	11/1809	28	36			19.6

TABLE 2. (*Continued*)

Location	Min sea level pressure		Max surface wind speed			Storm surge (m)[c]	Storm tide (m)[d]	Tot rain (mm)
	Date/time (UTC)	Pressure (mb)	Date/time (UTC)[a]	Sustained (kt)[b]	Gust (kt)			
Florida (unofficial)								
Apollo Beach								128.3
Bartow								135.4
Crystal River Power Plant						1.2		
Dixie County						1.5[e]	2.7[e]	
Four Corners								144.5
Hernando Beach						1.2[e]		
Lamont								128.0
Lithia								130.8
Mayo								127.5
Myakka Head 8 W								132.8
New Port Richey EOC					47			
Panacea								144.3
Pine Island						1.2[e]		
Plant City								135.9
Port Richey						1.2[e]		
Ruskin								171.7
Tarpon Springs 5 E								179.8
Taylor County						1.2[e]	2.4[e]	
Wares Creek								141.5
Wimauma 4 SW								140.5
Georgia								
Alma (KAMG)	14/0053	1002.6						51.1
Brunswick (KBQK)			13/2322		38			
Saint Simons Island NOS						0.3	2.3	
Savannah (KSAV)	14/0753	1007.0	14/0025	28	39			83.6
St. Simons Island (KSSI)	13/2253	1007.2	13/1953	21	35			21.6
Georgia (unofficial)								
Meridian					34			
Rincon								179.1
Savannah (downtown)					37			
Tybee Island					43			
Wilmington Island								136.4
South Carolina								
Charleston (KCHS)	14/1056	1006.3	14/1309	26	34			63.8
Charleston Harbor NOS						0.4	2.1	
Charleston (downtown) (KCHL)			14/0818	28	36			
Edisto Beach NWS Sensor					44			
Fort Pulaski NOS (FPKG1)			13/1718	29	37	0.3	2.6	
Fripps Inlet NOS (FRPS1)			13/2312	33	36	0.4	2.4	
South Capers Island NOS (SCIS1)	14/1112	1007.9	14/1054	30	38	0.4	2.0	
South Carolina (unofficial)								
Capers Island					38			
Edisto Beach Town Hall					42			
Folly Beach Town Hall					41			
Fripp Island					38			
Hilton Head					35			
Isle of Palms					37			
Pineville			14/1431	33	42			

TABLE 2. (*Continued*)

Location	Min sea level pressure		Max surface wind speed			Storm surge (m)[c]	Storm tide (m)[d]	Tot rain (mm)
	Date/time (UTC)	Pressure (mb)	Date/time (UTC)[a]	Sustained (kt)[b]	Gust (kt)			
Buoys/CMAN sites								
41004	14/1050	1009.3	14/1440	30[f]	41			
41008	13/2250	1008.1	14/0200	31[f]	43			
42003	12/0750	1002.9	12/1350	39[f]	49			
42013 University of South Florida (USF)	12/2210	1008.3	12/2210	29[f]	35			
42021 (USF)	13/0700	1004.5	13/0300	35	39			
42036	13/0250	995.8	13/1040	35[f]	45			
42039	12/2050	1005.4	12/2050	31	39			
Anclote Key (USF) (ANCF1)			13/1200	26	37			
Cedar Key (CDRF1)	13/0900	1004.1	18/0830	36[f]	48	1.3	2.1	
Egmont Key (USF) (EGKF1)			13/0054	31	39			
Folly Island (FBIS1)	14/1000	1008.6	14/1100	35	44			
Fred Howard (USF) (FHPF1)	13/0854	1006.1	13/0754	35	47			
Homosassa (USF) (HSSF1)	13/0754	1005.3	13/1754	33	42			
Keaton Beach (KTNF1)	13/1600	997.5	13/1820	32[f]	39			
Port Richey (USF) (PTRF1)	13/0854	1003.0	13/1154	29	35			
Pulaski Shoal Light (PLSF1)			11/0540	36[f]	47			
Sand Key (SANF1)			10/1740	32[f]	40			
Shell Point (USF) (SHPF1)	13/1054	1001.5						
St. Augustine (SAUF1)	13/2000	1008.7	13/0900	35	42			
Sunshine Skyway Bridge			13/0646	39	49			
Tyndall AFB Tower (SGOF1)	13/0800	1001.1	13/0540	45[f]	52			
U.S. Navy Tower M2R6 (SKMG1)	13/2233	1008.8	14/0333	36	43			
U.S. Navy Tower R2 (SPAG1)			14/0633	37	43			
U.S. Navy Tower R8 (TYBG1)	14/0826	1009.0	14/0426	31	41			
Venice (VENF1)	13/0800	1009.2	13/0640	36[f]	46			

[a] Date/time is for sustained wind when both sustained and gust are listed.
[b] Except as noted, sustained wind averaging periods for C-MAN and land-based Automated Surface Observing System (ASOS) reports are 2 min; buoy averaging periods are 8 min; and NOS averaging periods are 6 min.
[c] Storm surge is water height above normal astronomical tide level.
[d] Storm tide is water height above National Geodetic Vertical Datum (1929 mean sea level).
[e] Estimated.
[f] Ten-minute average.

foundland later on 18 July, then turned toward the east-northeast and dissipated on 19 July over the open waters of the North Atlantic Ocean. There were no reports of damage or casualties associated with this system.

While the low was considered to be a frontal cyclone operationally, postevent analysis of the system revealed no significant frontal boundaries. In particular, Canadian buoy 44137 indicated little or no surface temperature gradient across the cyclone as it passed close by, and a QuikSCAT pass at 2234 UTC 17 July showed no evidence of frontal structures in the wind field. The QuikSCAT data also showed that the system had a relatively small radius of maximum winds (about 30 n mi), and the buoy data indicated a steep drop in pressure and sharp increase in wind that are typical of a tropical cyclone. Figure 5 shows the system with a large burst of convection and the overall satellite appearance of a sheared tropical cyclone. AMSU observations, which were unavailable in real time, indicate that the system had a significant tropospheric warm core, and these observations are consistent with the Florida State University phase analysis (Hart 2003) of the system. Based on this evidence, the system is considered to have been a tropical cyclone.

c. Tropical Storm Beryl, 18–21 July

The genesis of Beryl can be traced to the same frontal system that spawned the unnamed tropical storm. The front stalled off the coast of North Carolina on 16 July, and over the next day or two the temperature gradient across the front gradually dissipated over sea surface temperatures of 26°–27°C. By 1200 UTC 18 July, a low pressure center formed near the southwestern end of the remnant trough, about 250 n mi east-southeast of Wilmington, North Carolina, with sufficient organized deep convection to designate the sys-

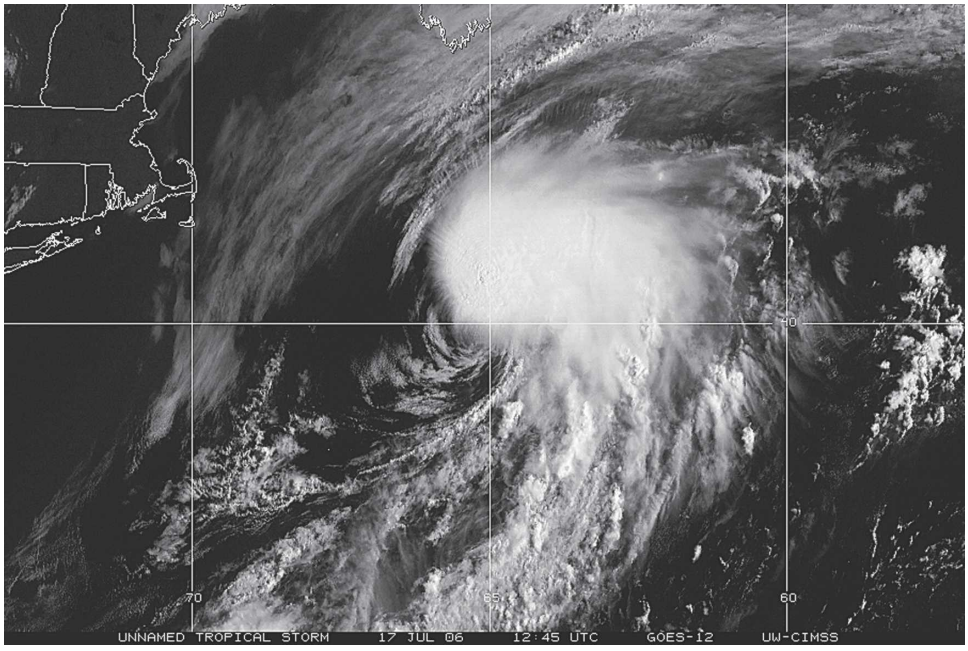

FIG. 5. *GOES-12* visible satellite image of the unnamed tropical storm at 1245 UTC 17 Jul 2006 (image courtesy of University of Wisconsin—Madison).

tem as a tropical depression. Six hours later, as convective banding features became more prominent over the eastern semicircle of the circulation, the cyclone became a tropical storm.

From 18–20 July, the tropical storm moved mainly northward, paralleling the coast of the mid-Atlantic states along the western periphery of a subtropical high pressure area. Vertical shear was not strong and upper-level anticyclonic outflow became established over the system, allowing Beryl to strengthen to its maximum intensity of 50 kt by 1800 UTC 19 July. Beryl maintained this intensity for about a day, but by 1800 UTC 20 July a slow weakening trend began as Beryl passed over cooler waters. Steering winds ahead of a midtropospheric trough moving through the Great Lakes caused the storm to turn toward the north-northeast and northeast, with a gradual increase in forward speed. The center of Beryl passed over Nantucket around 0645 UTC 21 July, at which time the cyclone's maximum sustained winds were estimated to be 45 kt. The cyclone continued to accelerate northeastward, and Beryl lost tropical characteristics shortly after 1200 UTC 21 July. The system crossed Nova Scotia and moved over Newfoundland, where it merged with another extratropical cyclone after 1200 UTC 22 July.

Selected surface observations associated with Beryl from land stations and data buoys are given in Table 3. Wind gusts to tropical storm force were reported on Nantucket. There were no reports of casualties or damage.

d. Tropical Storm Chris, 1–4 August

The tropical wave that spawned Chris moved across the west coast of Africa early on 26 July, and maintained vigorous convection for the next couple of days as it moved westward at 15–20 kt. By late on 28 July, the convection weakened considerably and became less organized as the system moved into a region of large-scale subsidence and dry air. The wave continued to propagate westward at a slightly slower forward speed, and convection began to increase on 30 July several hundred miles east of the southern Leeward Islands. The convection became better organized over the next day or so, and a closed surface wind circulation developed late on 31 July. It is estimated that a tropical depression formed at 0000 UTC 1 August about 205 n mi east-southeast of Barbuda.

The depression moved west-northwestward at about 10 kt, and despite moderate upper-level westerly wind shear, became a tropical storm around 0600 UTC 1 August. Chris reached its peak intensity of 55 kt early on 2 August about 55 n mi east-northeast of Anguilla in the northern Leeward Islands, but began to weaken the following day when northwesterly shear increased and dry air became entrained into the circulation. Chris passed about 100 n mi north of Puerto Rico and Hispaniola and weakened to a tropical depression at 1800 UTC 3 August, when the cyclone was centered about 195 n mi east-southeast of Grand Turk Island. Strong

TABLE 3. Selected surface observations for Tropical Storm Beryl, 18–21 Jul.

Location	Min sea level pressure		Max surface wind speed			Storm surge (m)[c]	Storm tide (m)[d]	Tot rain (mm)
	Date/time (UTC)	Pressure (mb)	Date/time (UTC)[a]	Sustained (kt)[b]	Gust (kt)			
			Massachusetts					
Chatham (KCQX)	21/0828	1003.1	21/0759	22	29			8.4
Hyannis (KHYA)	21/0806	1005.1	21/0658	20	26			5.3
Martha's Vineyard (KMVY)	21/0705	1005.5	21/0425	23	30			1.8
Nantucket (KACK)	21/0721	1000.4	21/0623	30	38	0.3		7.1
			Massachusetts (unofficial)					
Nantucket NWS Skywarn Spotter	21/0657	1000.4	21/0612		39			
Nantucket Sound Cape Wind Buoy (Horseshoe Shoal)		1006.0	21/0610	34	44			
			Buoys					
41630 (32.6°N, 76.3°W)	19/0900	1015.6	19/0900	39				
41645 (33.2°N, 71.6°W)	19/1600	1020.8	19/1600	43				
44008 (40.5°N, 69.4°W)			21/0550	35	49			
44018 (41.3°N, 69.3°W)	21/0900	1001.1	21/0800	33	43			

[a] Date/time is for sustained wind when both sustained and gust are listed.
[b] Except as noted, sustained wind averaging periods for C-MAN and land-based ASOS reports are 2 min; buoy averaging periods are 10 min.
[c] Storm surge is water height above normal astronomical tide level.
[d] Storm tide is water height above National Geodetic Vertical Datum (1929 mean sea level).

westerly shear continued, and the convection associated with Chris diminished as the system moved westward toward the southeastern Bahamas. Chris degenerated into a nonconvective remnant low pressure system by 0600 UTC 4 August about 80 n mi east-southeast of Grand Turk Island. The remnant circulation skirted the northern coast of Cuba before it dissipated on 6 August near Havana.

Direct effects from Chris in the Lesser and Greater Antilles were mainly confined to brief periods of heavy rainfall and some localized floods. News reports indicate rainfall from the storm caused the Fajardo River in Puerto Rico to overflow its banks. Rainfall reached up to 50 mm across portions of Hispaniola, the Turks and Caicos, the Bahamas, and eastern Cuba. In some of the mountainous areas of Hispaniola, there were unofficial reports of near 100 mm of rain. Although the center of Chris passed about 100 n mi to the north of the Dominican Republic, the cyclone still caused heavy rains and significant floods in and around Santo Domingo, where many roads were impassable due to the combined effects of high water and mudslides. Overall, however, damage was minor and no casualties were reported.

e. Tropical Storm Debby, 21–26 August

Debby formed from a vigorous tropical wave that moved across the west coast of Africa on 20 August. Almost immediately after moving offshore, the wave developed convective banding and a broad closed circulation. The first Dvorak classification was made at 1200 UTC 21 August, and by 1800 UTC a tropical depression had formed about 225 n mi south-southeast of Praia in the Cape Verde Islands.

The depression initially moved west-northwestward to the south of the subtropical ridge. Around 1200 UTC 22 August, the center of the cyclone passed about 100 n mi to the southwest of the southernmost Cape Verde Islands, bringing thunderstorms and gusty winds to the southern islands of Fogo and Brava. The depression strengthened as it moved away from the islands, becoming a tropical storm around 0000 UTC 23 August. By 1200 UTC that day, Debby's sustained winds reached 45 kt, but there was little or no change in strength for the next two days while the cyclone moved between west-northwestward and northwestward at 15–20 kt over the open waters of the eastern Atlantic. Intensification during this period appeared to be limited by a dry and stable air mass surrounding the cyclone, along with marginal sea surface temperatures. On 25 August, southerly shear increased in association with an upper-level trough, displacing the deep convection to the north of the center. Debby began to weaken and became a depression around 0600 UTC 26 August. By 1200 UTC that day there was no deep convection within about 150 n mi of the center, and Debby degenerated to a remnant low about 1225 n mi east-southeast

of Bermuda. The remnant low turned gradually northward ahead of an approaching frontal trough, generating intermittent convection before dissipating just east of the trough early on 28 August.

f. Hurricane Ernesto, 24 August–2 September

Ernesto, with landfalls as a tropical storm in Cuba, Florida, and North Carolina, was fleetingly a hurricane over the central Caribbean Sea. The storm also produced torrential rainfall and floods in portions of Hispaniola, while gale-force winds and heavy rains associated with the extratropical remnants of Ernesto affected portions of Virginia, Maryland, Delaware, and New Jersey. Ernesto was directly responsible for five fatalities in Haiti.

1) SYNOPTIC HISTORY

Ernesto formed from a tropical wave that emerged from the west coast of Africa on 18 August and moved steadily westward across the tropical Atlantic during the following several days. On 23 August, convection associated with the wave increased, triggering the first Dvorak classifications at 1200 UTC, when the wave was located about 500 n mi east of the Lesser Antilles. As the wave approached the Lesser Antilles, a surface low formed near the southern Windward Islands. The system soon acquired a well-defined surface circulation and became a tropical depression at 1800 UTC 24 August, while centered about 40 n mi north-northwest of Grenada.

Convection increased over the low-level center of the depression as it moved toward the west-northwest along the southern periphery of a midlevel ridge over the western Atlantic. The cyclone became a tropical storm at 1200 UTC 25 August while centered about 280 n mi south of San Juan, Puerto Rico. Ernesto turned toward the northwest and continued to intensify as it moved into the central Caribbean Sea on 26 August. The next day at about 0600 UTC, while Ernesto was centered about 70 n mi south of the southern coast of Haiti, it was very briefly of hurricane strength, with maximum sustained winds of 65 kt and a minimum pressure of about 992 mb. Shortly thereafter, the small inner core of the storm deteriorated as the circulation interacted with the mountainous terrain of Haiti, and Ernesto quickly weakened back to a tropical storm. The center of circulation passed offshore very near the southwestern tip of Haiti at about 0000 UTC 28 August, by which time the storm's intensity had decreased to 40 kt.

Under southwesterly shear associated with an upper-level low over the Bahamas, Ernesto continued to weaken as it moved northwestward toward Cuba. The storm had maximum sustained winds of 35 kt when its center made landfall along the southeastern coast of Cuba, near Playa Cazonal and just west of Guantanamo Bay, at 1115 UTC 28 August. Ernesto turned northwestward and its center stayed inland over Cuba for about 18 h, but it remained a tropical storm during that time. The center emerged off the north-central coast of Cuba by 0600 UTC 29 August and the intensity increased slightly to 40 kt. A midlevel high pressure area over the southeastern United States was migrating eastward during this period, allowing Ernesto to continue northwestward. The storm began to traverse the warm waters of the Florida Straits late on 29 August, and convection gradually increased. Apparently still hindered by disruption of its inner core over Cuba, and possibly influenced by moderate easterly wind shear, Ernesto did not gain any additional strength between Cuba and southern Florida.

Ernesto made landfall at Plantation Key, Florida, around 0300 UTC 30 August. Two hours later, a second landfall occurred on the Florida mainland in southwestern Miami–Dade County. At both landfalls Ernesto had maximum sustained winds of 40 kt and a minimum central pressure of 1003 mb. Thereafter, Ernesto weakened only slightly, and it remained a tropical storm throughout its passage over Florida. The storm moved northward along the center of the Florida Peninsula and within a weakness in the midlevel ridge, its center passing over Lake Okeechobee around 1800 UTC 30 August. Ernesto turned north-northeastward, and its center emerged over the Atlantic Ocean near Cape Canaveral, Florida, very early on 31 August.

Fueled by the warm waters of the Atlantic, convection increased over the center of the cyclone, and Ernesto intensified to a strong tropical storm as it continued north-northeastward ahead of a deep-layer trough approaching from the west. It reached an intensity of 60 kt by 1800 UTC 31 August while centered about 150 n mi south-southwest of Wilmington (Fig. 6). The central pressure continued to gradually fall, and an eye was becoming discernible in satellite imagery as the storm center approached the coast. The center came ashore at 0340 UTC 1 September on Oak Island, North Carolina, a few miles south-southwest of Wilmington and just west of Cape Fear. At the time of landfall, Ernesto was very near the threshold between tropical storm and hurricane status, with an intensity of 60 kt and a minimum pressure of 985 mb. Ernesto weakened as it moved across eastern North Carolina, where it became a tropical depression by 1200 UTC 1 September.

Even before Ernesto had reached North Carolina,

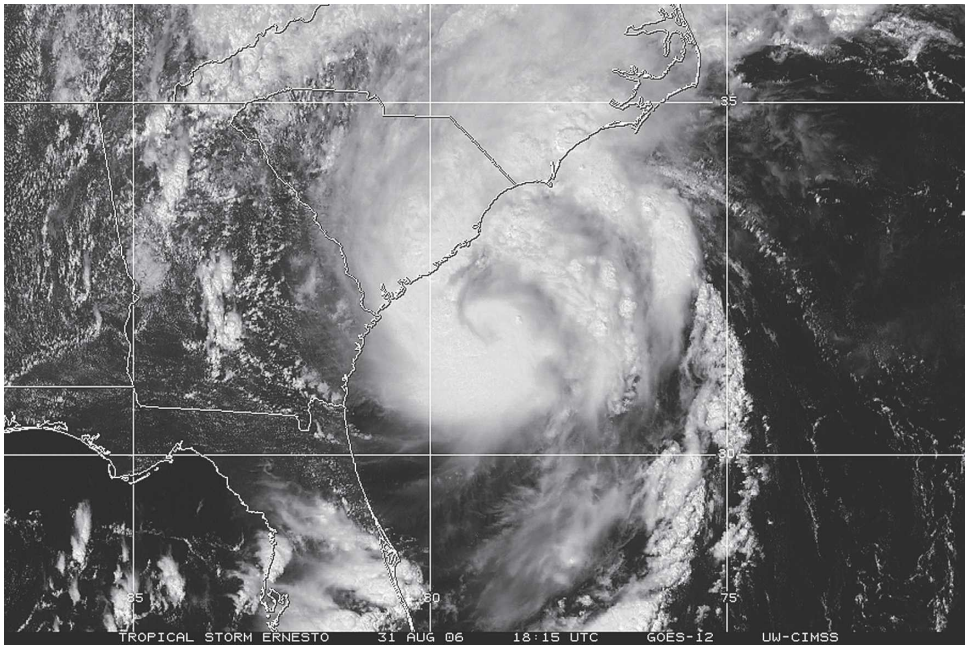

FIG. 6. *GOES-12* visible satellite image of Hurricane Ernesto (as a tropical storm) at 1815 UTC 31 Aug 2006 (image courtesy of University of Wisconsin—Madison).

the pressure gradient between the tropical cyclone and high pressure centered over southeastern Canada was producing gale-force winds near the coasts of Virginia, Maryland, Delaware, and New Jersey. These gales continued even after Ernesto weakened to a tropical depression. By the time the center of circulation reached the North Carolina–Virginia border at about 1800 UTC 1 September, Ernesto had interacted with a preexisting frontal zone and become extratropical. The extratropical remnant of Ernesto moved slowly northward over Virginia and Maryland on 2 September, with peak winds of about 40 kt. By 1800 UTC that day, when the center of circulation was near Washington, D.C., the system began to weaken. On 3 September, it was no longer producing gale-force winds as it accelerated across Pennsylvania and New York into southeastern Canada, and it was absorbed into a larger extratropical low pressure system the next day.

2) METEOROLOGICAL STATISTICS

Ernesto was briefly near the threshold between tropical storm and hurricane strength over the central Caribbean Sea early on 27 August. A dropsonde at 0832 UTC measured an instantaneous wind of 64 kt at 10 m, but poststorm analysis of the profile suggested that this observation was most likely representative of a gust rather than a sustained wind; the surface estimate derived from the mean wind over the lowest 150 m of this sounding was only 56 kt. The strongest flight-level wind measurement that day was 78 kt at 0732 UTC, corresponding to about 62 kt at the surface using the average adjustment from 850 mb (Franklin et al. 2003). One hour later, at 0834 UTC, the aircraft measured a flight-level wind of 69 kt at 700 mb, which also corresponds to about 62 kt at the surface. Given the inability of the aircraft to sample the entire circulation, it is possible that during this period somewhat stronger winds occurred elsewhere that would be consistent with the operational estimate of Ernesto briefly having 65 kt winds near 0900 UTC 27 August.

Ernesto's estimated Florida landfall intensity of 40 kt is based on aircraft observations. The strongest sustained surface wind measured in Florida was 35 kt, obtained by an instrument on Lake Okeechobee operated by the South Florida Water Management District (SFWMD), at 2030 UTC 30 August (Table 4). The Lake Worth Coastal-Marine Automated Network (C-MAN) station, on the Atlantic coast in Palm Beach County, also reported a sustained wind of 35 kt that day. These data suggest that Ernesto remained a tropical storm throughout its entire path over Florida, although the only areas to receive sustained winds of tropical storm force likely were near or over water.

Ernesto was again near the threshold between tropical storm and hurricane status near the time of landfall in North Carolina. The strongest flight-level (850 mb) wind on 31 August was 73 kt at 1947 UTC, corresponding to about 58 kt at the surface. The SFMR instrument

measured 60–65 kt near 1800 UTC, but the higher end of this range resulted from isolated peak values that appeared slightly inflated by rain and were therefore discounted. Radar velocities measured from the Weather Surveillance Radar-1988 Doppler (WSR-88D) at Wilmington reached 80–84 kt at an altitude of 1500 ft just west of the circulation center less than 3 h prior to landfall, corresponding to about 60–63 kt at the surface, but the highest values were associated with a transient, mesoscale feature. Although the best-track intensity during this period was set to 60 kt, it is possible that the maximum wind was not sampled and that Ernesto might have reached hurricane strength near North Carolina.

The lowest central pressure of 985 mb occurred near the time of final landfall, as evidenced by a surface observation of 985.4 mb at Wilmington. The central pressure remained relatively low as Ernesto proceeded inland. Six hours after landfall, when the center was about 90 n mi inland, a pressure of 988.5 mb was measured at Kinston, North Carolina. The strongest sustained wind measured by an official surface-based anemometer in North Carolina was 50 kt at the Wrightsville Beach NOS station at Johnny Mercer Pier, where a gust to 64 kt was also reported. An unofficial gust to 79 kt was reported at Cedar Island, just northeast of Cape Lookout. The storm surge produced by Ernesto was just less than 1 m, although a total water rise (storm tide) of nearly 2 m was reported in a few locations. The surge affected a long stretch of the North Carolina coastline, including the bays, harbors, and rivers adjacent to Pamlico Sound as far north as Dare County (Table 4).

The interaction of Ernesto with high pressure centered over southeastern Canada produced sustained gale-force winds and heavy rains over and near the coasts of Virginia, Maryland, Delaware, and New Jersey. Some of the observations included in Table 4 are associated with this interaction and are therefore not reflected in the best-track intensity of the tropical cyclone. The combined effects of the two systems, as well as the extratropical remnant of Ernesto, resulted in storm surge flooding along the western shores of Chesapeake Bay and the adjacent rivers, where storm tides of up to about 2 m were reported.

Storm-total rainfall amounts exceeded 125 mm throughout a broad swath across eastern South Carolina, North Carolina, and Virginia, as well as southern Maryland (Table 4). More than 250 mm of rain fell in several locations in North Carolina and Virginia, including a maximum of 371 mm at Wrightsville Beach, North Carolina. The heavy rains also led to river flooding for several days after Ernesto's landfall. In particular, the Northeast Cape Fear River crested at 5.7 m at Chinquapin, well north of Wilmington, and remained in major flood stage from 2–7 September.

The large metropolitan areas of southeastern Florida escaped with no more than 25–50 mm of rain from Ernesto. The storm dropped 75–150 mm of rain, however, in many areas near the path of the storm's center from the Cape Canaveral area to Lake Okeechobee, in portions of southwestern Florida, and in isolated spots in the upper Florida Keys. A storm-total maximum of 221 mm was reported at the South Golden Gate Estates SFWMD station located east of Naples. In the Caribbean, 75–125 mm of rain were common over much of eastern Cuba as Ernesto moved over the island, with a maximum of 189 mm reported at Nuevitas, Camaguey. In the Dominican Republic, 178 mm of rain fell at Barahona as the center of Ernesto passed to the southwest.

A total of five weak tornadoes were reported in association with Ernesto. Two of these touched down in Osceola County in central Florida on the afternoon of 30 August, and the other three were reported in eastern North Carolina on the evening of 31 August.

3) CASUALTY AND DAMAGE STATISTICS

Ernesto was directly responsible for five fatalities, all in Haiti. In addition, the extratropical remnant of Ernesto was responsible for two deaths that occurred in Gloucester, Virginia, when a tree fell on a residence.

In the Caribbean, Ernesto was associated with damage in Haiti, the Dominican Republic, and Cuba. Ernesto caused mudslides and flooded many residences across the mountainous terrain of Hispaniola. At least six homes were destroyed with dozens more damaged in Haiti, and a bridge was destroyed in Port-au-Prince. More than 400 homes were flooded in the city of Santo Domingo in the Dominican Republic. Only minor damage was reported in Cuba.

The estimate of insured losses in the United States, provided by the Property Claim Services of the Insurance Services Office, is $245 million. Total U.S. property damage is estimated at roughly $500 million. In eastern North Carolina, heavy rains resulted in the flooding of several homes, and other homes were damaged by strong winds. For days following landfall, rain-induced river flooding inundated several homes along the Northeast Cape Fear River north of Wilmington. Storm surge caused minor coastal flooding and beach erosion along the immediate Atlantic coastline. The surge along bays and rivers, including the Pamlico and Pungo Rivers in Beaufort County and Collington Harbor in Dare County, flooded several homes and businesses. Minor property damage was caused by the three tornadoes in eastern North Carolina. In Virginia, storm

TABLE 4. Selected surface observations for Hurricane Ernesto, 24 Aug–1 Sep 2006. The table includes observations indirectly associated with Ernesto as well as during Ernesto's extratropical stage.

Location	Min sea level pressure		Max surface wind speed			Storm surge (m)[c]	Storm tide (m)[d]	Tot rain (mm)
	Date/time (UTC)	Pressure (mb)	Date/time (UTC)[a]	Sustained (kt)[b]	Gust (kt)			
Puerto Rico								
Sabana Grande ALERT								119.1
Dominican Republic								
Barahona (MDBH)	28/2100	1011.2						178.1
Las Americas (MDSD)	27/0900	1012.0						104.9
Cuba								
Contramaestre, Santiago de Cuba (78363)								89.9
Gran Piedra, Santiago de Cuba (78366)								101.3
Guantánamo (78334)								139.7
Guantánamo (78356)								107.4
Guantánamo (78368)								136.9
Nuevitas, Camagüey (78353)			28/2015		45			189.5
Palo Seco, Camagüey (78354)								83.3
Pinares de Mayari, Holguín (78371)								72.9
Punta de Maisi, Guantánamo (78369)								130.3
Punta Lucrecia, Holguín (78365)			28/1715		49			86.6
Universidad, Santiago de Cuba (78364)								91.4
Velasco, Holguín (78378)								79.0
Florida								
Cache Remote Automated Weather Station (RAWS)			30/1015		38			89.4
Chekika (CHKF1)			30/1235		37			
Clearwater Beach NOS (CWBF1)			30/2230	22	43			
Fort Lauderdale (KFLL)	30/1312	1004.7	30/1312	25	37			32.0
Fort Lauderdale Executive Airport (KFXE)	30/1353	1005.3	30/1731	26	34			18.5
Fort Pierce (KFPR)	30/2201	1002.0	30/1717	26	34			28.4
Homestead (KHST)	30/0655	1004.5	29/1655	22	33			
Key West (KEYW)	30/0942	1008.1	30/1008	25	34			34.3
Marathon (KMTH)	30/0910	1007.1	30/0839	23	28			80.8
Melbourne (KMLB)	30/2339	1001.0	31/0213	25	32			77.7
Melbourne National Weather Service Forecast Office (NWSFO)								88.1
Miami (KMIA)	30/1153	1004.6	30/1257	22	32			18.3
Miles City (RAWS)								169.9
Naples Pier NOS (NPSF1)			30/2154		43	0.3	0.9	
Opa-Locka (KOPF)	30/1153	1004.3	30/1315	30	35			8.6
Pembroke Pines (KHWO)	30/1335	1005.1	30/1253	23	37			34.3
Pompano Beach (KPMP)	30/1353	1005.5	30/1238	29	40			21.8
Vaca Key NOS (VACF1)			30/0842	26	43	0.3	0.5	
Vero Beach (KVRB)	30/2224	1001.7	30/2027	27	34			38.4
Virginia Key NOS (VAKF1)			30/1300		39	0.3	0.9	
West Kendall (KTMB)	30/1116	1003.7	30/0638	22	32			38.9
West Palm Beach (KPBI)	30/1837	1006.1	30/1336	28	37			33.0
Florida (unofficial)								
Archbold Bio Station								151.6
Big Pine Key (NWS Employee)								116.6
Boca Raton			30/1230		44			
Boynton Beach	30/1351	1005.1	30/1351		36			
Chokoloskee (CHOF1)								124.5
Delray Beach			30/1423		36			
Devils Garden (DVLF1)								121.9
East Golden Gate								136.4

TABLE 4. (*Continued*)

Location	Min sea level pressure		Max surface wind speed			Storm surge (m)[c]	Storm tide (m)[d]	Tot rain (mm)
	Date/time (UTC)	Pressure (mb)	Date/time (UTC)[a]	Sustained (kt)[b]	Gust (kt)			
Florida (unofficial)								
Immokalee (IMKF1)								151.4
Jensen Beach			30/2326		40			24.6
Melbourne								102.1
Moore Haven (MHVF1)								121.4
NE Lehigh Acres								111.3
Ortona (ORTF1)								107.4
SFWMD stations								
Big Cypress Station								123.2
Big Cypress Station 14								160.3
Big Cypress Station 17								131.3
Fakahatchee Strand								212.6
Hendry Landfill								119.6
Immokalee Landfill								147.6
Lake Okeechobee L001			30/1945	23[e]	36			
Lake Okeechobee L005			30/2000	34[e]	51			
Lake Okeechobee L006			30/1900	25[e]	31			
Lake Okeechobee LZ40			30/2030	35[e]	45			
Loxahatchee			30/1745	24[e]	35			
Palmdale								157.2
S331W			30/1245		34			
S7WX			30/1645		32			
South Golden Gate								221.5
South Carolina								
Charleston Harbor						0.3	1.9	
Fripps Inlet NOS (FRPS1)	31/2012	1009.2				0.2	2.0	
Myrtle Beach (KMYR)	01/0150	998.3	01/0050	30	40			
North Myrtle Beach (KCRE)	01/0459	995.9	01/0147	22	35			183.4
South Capers Island NOS (SCIS1)						0.4	1.9	
Springmaid Pier NOS (MROS1)	01/0200	998.0	31/1700	26	38			
South Carolina (unofficial)								
Conway								102.1
Daniel Island								114.3
McClellanville								161.3
Mount Pleasant								173.2
Myrtle Beach FD6								160.0
North Carolina								
Beaufort (KMRH)	01/1156	1003.0	01/0938	37	45			120.9
Cape Hatteras (KHSE)	01/1033	1004.7	01/0930	38	44			116.1
Cherry Point MCAS (KNKT)	01/0914	998.0	01/0509	34	44			101.9
Clinton (KCTZ)					38			
Coastal Onslow and Carteret County						0.6–0.9[f]		
Dare County (Collington Harbor)						0.9[f]		
Duck							1.3	
Eastern Pamlico County						0.3–0.6[f]		
Elizabeth City (KECG)	01/0654	1012.1	01/0854	29	36			
Elizabeth City Coast Guard Station								128.8
Elizabethtown (KEYF)	01/0700	995.9	01/0742	22				111.3
Fayetteville (KFAY)	01/0653	999.8	01/0525	29	42			54.1
Fort Bragg (KFBG)	01/0755	1001.5	01/0555	17	35			
Goldsboro (KGWW)					39			
Greenville (KPGV)	01/1140	992.9	01/0920	26	39			
Henderson (KHNZ)					34			

TABLE 4. (*Continued*)

Location	Min sea level pressure		Max surface wind speed			Storm surge (m)[c]	Storm tide (m)[d]	Tot rain (mm)
	Date/time (UTC)	Pressure (mb)	Date/time (UTC)[a]	Sustained (kt)[b]	Gust (kt)			
North Carolina								
Holly Shelter Back Island (RAWS)								259.3
Jacksonville (KOAJ)	01/0815	988.1	01/0815	32	46			171.5
Kenansville (KDPL)	01/0821	989.8	01/0701	32	51			
Kinston (KISO)	01/0940	988.5	01/0840	25	38			
Louisburg (KLHZ)					34			
Maxton (KMEB)					36			30.7
New Bern (KEWN)	01/0922	996.2	01/0950	31	51	0.8		142.2
New Bern (RAWS)								104.9
New River MCAS (KNCA)	01/0808	992.2	01/0705	41	51			132.8
Newport-Croatan (RAWS)								155.4
Roanoke Rapids (KRZZ)	01/1454	998.2	01/1304	24	39			97.8
Rocky Mount/Wilson (KRWI)	01/1053	995.6	01/0825	29	40			94.7
Sandy Run (RAWS)								144.3
Seymour-Johnson AFB (KGSB)	01/0955	991.5	01/.755	28	46			
Southport (KSUT)	01/0340	987.8	01/0040	23	43			
Supply (RAWS)								185.2
Turnbull Creek (RAWS)								113.0
Washington (KOCW)	01/1202	995.3	01/1202	24	40		1.2–1.8[f]	
Whiteville (RAWS)								114.8
Wilmington (KILM)	01/0447	985.4	01/0335	36	54			244.9
Wrightsville Beach NOS (JMPN7)	01/0436	986.8	01/0330	50	64	0.9	1.8	
North Carolina (unofficial)								
Aurora Environmental and Climate Observing Network (ECONET)			01/1100	23				134.1
Bunyan 3ESE (BNYN7)								128.3
Burgaw 3W								218.4
Castle Hayne ECONET			01/0353	30				241.0
Cedar Island (CITN7)	01/1010	1002.0	01/1210		79			
Clinton								116.8
East Arcadia								185.9
Goldsboro								115.3
Goldsboro 5E (Spotter)								134.6
Greenville (PGVN7)								176.8
Grifton								250.2
Hampsted								282.7
Jacksonville 6NE (HFMN7)								135.6
Kinston (ECONET)			01/0700	21				206.0
Kinston (COOP)								243.1
Leland (NWS Employee)								215.9
Lewiston ECONET			01/0900	16				155.2
Longwood								194.3
Morehead City Fire Department (FD)					53			
Ocracoke					43			
Onslow Beach (RSLN7)			01/0955		59			
Pea Island (PEIN7)			01/1010		47			
Perrytown (PYTN7)								127.0
Richlands (RILN7)								179.3
Rocky Mount ECONET			01/1000	20				151.6
Snow Hill 8NE (LZZN7)								136.7
Southport (NC State Pilot)					59			
Stumpy Point (SPON7)			01/1000		43			
Sunny Point					59			
Sunny Points								131.6
Surf City Island								302.8
Surf City Mainland								218.7

TABLE 4. (*Continued*)

Location	Min sea level pressure		Max surface wind speed			Storm surge (m)[c]	Storm tide (m)[d]	Tot rain (mm)
	Date/time (UTC)	Pressure (mb)	Date/time (UTC)[a]	Sustained (kt)[b]	Gust (kt)			
North Carolina (unofficial)								
Swanquarter (SWQN7)	01/1200	1002.0	01/1210		46			
Tarboro (COOP)								147.3
UNC at Wilmington								230.4
Wallace (WCEN7)								203.2
Washington (TRAN7)								171.5
Wenona 7E (POCN7)								113.5
Whiteville 5S								115.6
Wilmington 7N								261.9
Wilmington/Kings Grant (NWS Employee)								248.9
Wilson (COOP)								118.1
Wrightsville Beach/Parmele Isle								371.1
Virginia								
Charlottesville (KCHO)								57.4
Chesapeake Bay Bridge Tunnel NOS CBBV2)							1.7	
Kiptopeke NOS (KPTV2)			01/1248	30	44		1.8	
Langley AFB (KLFI)	01/1855	1001.4	01/1243	41	58			184.2
Lewisetta NOS (LWTV2)			01/1800	37	55		1.7	
Melfa (KMFV)			01/1442	34	47			
Newport News (KPHF)	01/1755	1000.6	01/1345	39	48			214.9
Norfolk (KORF)	01/1751	1001.3	01/1153	36	46			229.9
Norfolk NAS (KNGU)	01/1753	1001.8	01/1145	36	48			168.1
Rappahannock Light NOS (RPLV2)			01/1812	48	58			
Richmond (KRIC)	01/2054	1004.3	01/1854	26	37			99.3
Rudee Inlet							1.9	
Sewells Point NOS (SWPV2)							1.7	
Virginia Beach–Oceana NAS (KNTU)	01/1856	1002.1	01/1111	29	45			145.0
Wakefield (KAKQ)	01/1954	1000.9						168.1
Wallops Island (KWAL)	01/2054	1006.1	01/2131	49	59			115.1
Washington Dulles (KIAD)								82.0
Washington Reagan National (KDCA)								68.8
West Point (KFYJ)			01/1642	27	54			
Windmill Point							1.6	
York River East Rear Range Light NOS YKRV2)			01/1318	52	66			
Yorktown NOS (YKTV2)			01/1436	52	65		1.8	
Virginia (unofficial)								
Amelia County								167.4
Carson								195.6
Central Garage								127.0
Charles City								158.0
Chesapeake								226.8
Chester								111.8
Chincoteague								203.2
Courtland								146.1
Disputanta								129.5
Fife								101.6
Gwynns Island								203.2
Hampton								177.8
Haymarket								101.6
Hopewell								105.4
Jamestown								209.6
King George								196.9
Little Plymouth								235.0

TABLE 4. (*Continued*)

Location	Min sea level pressure		Max surface wind speed			Storm surge (m)[c]	Storm tide (m)[d]	Tot rain (mm)
	Date/time (UTC)	Pressure (mb)	Date/time (UTC)[a]	Sustained (kt)[b]	Gust (kt)			
Virginia (unofficial)								
Louisa								109.2
Mangohick								190.5
Newland								114.3
Norfolk								254.0
Portsmouth								180.6
Reedville								106.7
Richmond (WTVR-TV)								145.5
Richmond (WWBT-TV)								106.7
Ruther Glen								120.7
Stanley								120.7
Tappahannock								114.3
Toano								221.7
Virginia Beach–Glenwood								246.1
Virginia Beach–Sandbridge								233.7
Virginia Beach–Thoroughgood								264.9
Warsaw								132.1
Waterfall								117.1
Weems								203.2
Windsor								193.8
Yale								190.5
Maryland								
Baltimore/Washington International (KBWI)								92.2
Beaverdam Creek							0.9	
Bishops Head NOS (BISM2)			01/2030	38	65		1.2	
Cambridge NOS (CAMM2)			02/0000	36	49		1.3	
Chesapeake City NOS (CHCM2)	02/0930	1010.9	02/0536	23	34			
Francis Scott Key Bridge NOS (FSKM2)	02/0930	1008.8	02/0300	28	35			
Ocean City Inlet							1.3	
Salisbury (KSBY)			01/2135	39	54			142.2
Solomons Island NOS (SLIM2)	01/2218	1007.9	01/2218	33	53			
Maryland (unofficial)								
American Corner								139.7
Annapolis								121.9
Baltimore								127.0
Federalsburg								124.5
Hollywood								175.8
Princess Anne								149.9
Snow Hill								182.6
Delaware								
Delaware City NOS (DELD1)	02/1000	1008.7	02/1000	29	40			
Dover AFB (KDOV)			02/0355		53			70.4
Georgetown (KGED)			02/0315					114.6
Lewes NOS (LWSD1)	02/0712	1008.5	02/0336	46	58			
Wilmington (KILG)			02/0451		41			44.2
Delaware (unofficial)								
Bethany Beach Boardwalk								103.1
Jones Crossing								130.8
Long Neck								114.3
Milford								114.3
Redden								114.8

TABLE 4. (*Continued*)

Location	Min sea level pressure		Max surface wind speed			Storm surge (m)[c]	Storm tide (m)[d]	Tot rain (mm)
	Date/time (UTC)	Pressure (mb)	Date/time (UTC)[a]	Sustained (kt)[b]	Gust (kt)			
New Jersey								
Belmar-Farmingdale (KBLM)			02/0835	29	39			
Cape May (KWWD)			01/2055	25	41			
McGuire AFB (KWRI)			02/1255	24	38			
Millville (KMIV)			02/0554	26	40			
Newark (KEWR)			02/1711	23	37			
Teterboro (KTEB)			02/1851	24	36			
Trenton (KTTN)			02/1100	23	35			
Buoys/C-MAN Sites								
41002			01/0400	30	45			
41004	31/1950	995.6	31/2200	41[g]	54			
41008	31/1050	1004.9	31/1610	26	31			
41012	31/0850	1000.3	31/1150	29	33			
41013	01/0150	990.5	01/0050	45[g]	56			
41025	01/1000	1003.9	01/1157	35	49			
41035	01/0700	993.7	01/0607	40	55			
44009	02/0650	1008.0	01/2350	39	49			
Ambrose Light, NY (ALSN6) (40.5N, 73.8W)			02/1110	44	52			
Cape Henry (CHLV2)	01/1900	1001.2	01/1342	50	57			
Cape Lookout (CLKN7)	01/0800	1002.2	01/0840	43	55			
Duck (DUCN7)	01/1730	1003.7	01/1107	36	50			
Folly Beach (FBIS1)	31/2000	1003.6	31/1400	25[g]	32			
Fowey Rocks (FWYF1)	30/0700	1006.0	30/0710	42	50			
Lake Worth (LKWF1)	30/1500	1005.9	30/1440	35	43			
Long Key (LONF1)	30/0400	1005.4	30/0850	33[g]	52			
Molasses Reef (MLRF1)	30/0300	1004.1	30/0530	34[g]	42			
Sand Key (SANF1)			30/1000	31	35			
Sombrero Key (SMKF1)	30/0600	1006.9	30/0600	33[g]	38			
Sunset Beach Carolinas Coastal Ocean Observing and Prediction System (Caro-COOPS)	01/0300	991.5	01/0100	32	43	0.5		
Thomas Point, MD (TPLM2) (38.9N 76.4W)	02/0700	1008.2	01/2200	41	46			
U.S. Navy Tower M2R6 (SKMG1)			31/1932	37	41			
U.S. Navy Tower R2 (SPAG1)			31/1400	33	37			

[a] Date/time is for sustained wind when both sustained and gust are listed.
[b] Except as noted, sustained wind averaging periods for C-MAN and land-based ASOS reports are 2 min; buoy averaging periods are 8 min; and NOS observations averaging periods are 6 min.
[c] Storm surge is water height above normal astronomical tide level.
[d] Storm tide is water height above National Geodetic Vertical Datum (1929 mean sea level).
[e] Fifteen-minute average.
[f] Estimated.
[g] Ten-minute average.

surge along the western shores of the Chesapeake Bay and into tidal sections of adjacent rivers flooded several homes, and some piers and boats were significantly damaged. Strong winds downed trees and power lines in coastal areas of North Carolina, Virginia, Delaware, and New Jersey. Ernesto's heavy rains in southwestern Florida caused flooding in several homes in Glades County.

g. Hurricane Florence, 3–12 September

Florence had a complex genesis that involved two tropical waves, the first of which moved across the west coast of Africa on 29 August. This wave moved slowly westward, showing some signs of convective organization on 31 August, when a second wave moved westward into the Atlantic at a faster forward speed. By 2

TABLE 5. Selected surface observations for Hurricane Florence, 3–12 Sep.

Location	Min sea level pressure		Max surface wind speed			Storm surge (m)[c]	Storm tide (m)[d]	Tot rain (mm)
	Date/time (UTC)	Pressure (mb)	Date/time (UTC)[a]	Sustained (kt)[b]	Gust (kt)			
Bermuda								
Bermuda Airport (TXKF; elevation 12 m MSL)		985.3	11/1602	57	78			33.5
Commisioner's Point (elevation 30 m MSL)			11/1400	67	95			
Esso Pier	11/1500	983.8	11/2000	38	61			
Fort Prospect (elevation 70 m MSL)			11/1340	49	82			
Maritime Operations Centre (elevation 78 m MSL)		980.8	11/1001		100			
St. David's (elevation 48 m MSL)			11/1340	71	97			

[a] Date/time is for sustained wind when both sustained and gust are listed.
[b] Except as noted, sustained wind averaging periods for C-MAN and land-based ASOS reports are 2 min; buoy averaging periods are 8 min; and NOS observations averaging periods are 6 min.
[c] Storm surge is water height above normal astronomical tide level.
[d] Storm tide is water height above National Geodetic Vertical Datum (1929 mean sea level).

September, the two waves combined to form a large area of disturbed weather over the eastern tropical Atlantic. The convective organization of the combined disturbance increased, and it is estimated that a tropical depression formed near 1800 UTC 3 September about 855 n mi west of the Cape Verde Islands.

With multiple vorticity maxima rotating around a mean center of circulation for several days, the depression's initial structure did not favor rapid development. In addition, southwesterly vertical shear associated with an upper-level trough to the system's west hindered development, and the depression took two days to reach storm strength as it moved west-northwestward. However, the shear decreased on 8 September when an upper-level ridge developed over Florence, and late that day convection began to consolidate around a vorticity center on the western side of the large cyclonic envelope. Florence strengthened slowly on 9 September and more rapidly the following day, becoming a hurricane early on 10 September about 340 n mi south of Bermuda.

Florence turned northward and reached its estimated peak intensity of 80 kt late on 10 September, but had weakened slightly when its center passed about 50 n mi west of Bermuda on 11 September. The hurricane recurved northeastward into the westerlies the next day, maintaining hurricane strength until it became extratropical early on 13 September about 420 n mi south-southwest of Cape Race, Newfoundland.

The extratropical remnant of Florence maintained a large circulation and hurricane-force winds as it approached Newfoundland. The center passed near Cape Race late on 13 September, then moved east-northeastward over the open North Atlantic before turning eastward and weakening on 14 September. After making a large cyclonic half-loop from 16–19 September southwest of Iceland, the remnant extratropical low was absorbed by a developing extratropical system to its south.

Florence brought hurricane conditions to Bermuda on 11 September (Table 5). An automated station at St. David's (elevation 48 m) reported sustained winds of 71 kt at 1340 UTC with a gust to 97 kt. The Bermuda Maritime Operations Centre reported a wind gust of 100 kt at 1001 UTC. The Bermuda Airport reported a peak gust of 78 kt at 1555 UTC along with 34 mm of rain. The extratropical remnant of Florence brought hurricane-force winds to portions of Newfoundland on 13 September, where Sagona Island reported sustained winds of 66 kt with a gust to 81 kt at 1500 UTC.

Media reports indicate that Florence caused no deaths on Bermuda and only a few minor injuries. The hurricane caused minor wind damage and power outages on the island. Minor wind damage and power outages also occurred in Newfoundland.

h. Hurricane Gordon, 10–20 September

Gordon, a category 3 hurricane at its peak, affected the Azores as a hurricane, and as an extratropical low brought heavy rains and high winds to parts of western Europe. The cyclone originated from a tropical wave that left the west coast of Africa on 2 September. This wave was initially well organized, with an associated surface low along the wave axis and some convection. However, vertical wind shear from an upper-level trough east of then Tropical Storm Florence hindered development for about a week as the wave and trough both progressed westward. By 9 September, the vertical

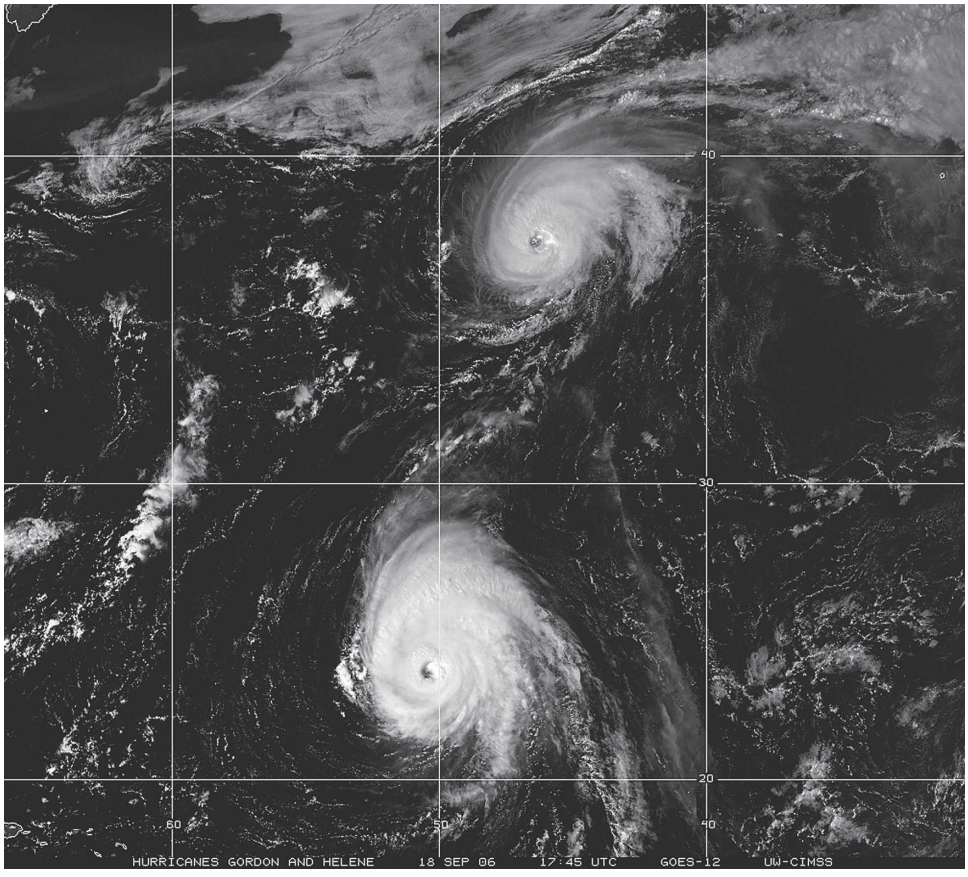

FIG. 7. *GOES-12* visible satellite image of Hurricanes Gordon and Helene at 1745 UTC 18 Sep 2006 (image courtesy of University of Wisconsin—Madison). Gordon is located at the top of the image.

shear in the vicinity of the tropical wave lessened slightly, and convection increased around the surface low. It is estimated that a tropical depression formed at 1800 UTC 10 September about 470 n mi east-northeast of the Leeward Islands.

The depression moved west-northwestward initially, and became a tropical storm the next day. Gordon turned toward the northwest and slowed on 12 September as it headed into a weakness in the subtropical ridge left behind Florence. The upper trough, which had continued to produce moderate southwesterly shear over the cyclone during this time, weakened and moved to the southwest, allowing the shear to abate. The storm turned toward the north and intensified into a hurricane, forming a large ragged eye early on 13 September. Gordon then rapidly intensified, its peak winds increasing by 50 kt in the 30-h period from 1800 UTC 12 September until 0000 UTC 14 September, and reached its estimated peak intensity of 105 kt while centered about 500 n mi east-southeast of Bermuda.

Gordon turned toward the northeast and briefly accelerated on 14 September, but an upper trough that had been steering the system bypassed the hurricane late that day. Midtropospheric ridging rebuilt to the north of Gordon and its forward motion stalled on 15 September, about 575 n mi east-southeast of Bermuda. Increasing vertical wind shear and the upwelling of cooler waters then caused Gordon to weaken to a category 1 hurricane on 16 September as it drifted northwestward.

Early on 17 September, building high pressure to the east of Gordon caused the hurricane to begin moving northeastward. Gordon accelerated to the northeast on 18 September, and turned to the east-northeast later that day around the strengthening subtropical high (Fig. 7). Vertical wind shear relaxed during this time and convection redeveloped around the eye. Despite moving over relatively cool waters of about 25°C, the cyclone reached a second peak intensity of 90 kt on 19 September about 420 n mi west-southwest of the Azores. Below-normal upper-tropospheric temperatures over the subtropical Atlantic likely countered the effects of the cool waters for a time, but later that day wind shear increased and Gordon began to weaken.

The hurricane moved a little south of due east early on 20 September, its center passing between the islands of São Miguel and Santa Maria in the Azores at about 0900 UTC. Hurricane-force wind gusts were experienced on Santa Maria, but Gordon's strongest winds remained south of the islands. Later that day, Gordon began interacting with a cold front and weakened, and the system became extratropical at 0000 UTC 21 September about 240 n mi west of the west coast of Portugal.

The extratropical remnant of Gordon was a vigorous system, maintaining winds of 55 kt or greater for almost two days after losing tropical characteristics. The extratropical low turned northeastward and was then driven northward at almost 50 kt on 21 September around a larger midlatitude low. Gordon's remnant remained distinct from the larger system, bringing heavy rains and winds gusts of hurricane-force to Spain and the United Kingdom, and on 22 September sustained winds with the system increased to hurricane force. Gordon's extratropical remnant became the dominant low pressure area and made a large cyclonic loop while slowly weakening over the far northeastern Atlantic Ocean. The system completed the loop just south of Ireland on 24 September and the low dissipated between Ireland and England later that day.

Observations of interest in Gordon include a peak wind gust of 71 kt, recorded at Santa Maria in the Azores on 20 September. The extratropical remnant of Gordon produced numerous gusts of hurricane force in Spain on 21 September, including one gust to 99 kt on the northwest coast at Punta Candieira. The British Broadcasting Corporation reported that wind gusts to 70 kt were measured in southwestern England, but no exact location was given.

There were no reports of casualties associated with Gordon as a tropical cyclone. The BBC reported only minor damage in the Azores, consisting mostly of fallen trees and power outages. After Gordon became an extratropical low, however, four injuries due to falling debris from high wind were reported in Spain. Power was also reported out for 100 000 customers in Spain. The extratropical cyclone brought high winds and rain that affected practice rounds at the Ryder Cup golf tournament in Ireland. About 126 000 homes were without power after the storm in Northern Ireland and one injury was reported.

i. Hurricane Helene, 12–24 September

Helene developed from a vigorous tropical wave and broad area of low pressure that emerged from the coast of Africa on 11 September. Convective activity associated with the low quickly increased, and by 1200 UTC 12 September the system had developed into a tropical depression while centered approximately 200 n mi south-southeast of the Cape Verde Islands. Under easterly shear, the sprawling depression was slow to develop initially. On 13 September, however, convective banding began to increase over the northwestern semicircle of the circulation and the depression became a tropical storm at 0000 UTC 14 September about 425 n mi west-southwest of the Cape Verde Islands.

Moving west-northwestward over the tropical Atlantic Ocean, Helene steadily intensified and became a hurricane at 1200 UTC 16 September about 1000 n mi east of the northern Leeward Islands. The next day Helene turned northwestward and slowed down in response to a weakness in the subtropical ridge created by Hurricane Gordon, which at that time was located a little over 1000 n mi northwest of Helene. Helene continued to strengthen, attaining category 3 status at 0000 UTC 18 September, and 6 h later it reached its estimated peak intensity of 105 kt. At this time, Helene and Gordon were at nearly the same longitude, with Gordon centered about 875 n mi north of Helene.

Helene had developed a concentric eyewall structure, and it weakened to a category 2 hurricane when the inner eyewall began to deteriorate late on 18 September (Fig. 7). As Gordon moved east of Helene's longitude, a narrow mid- to upper-level ridge built to the north of Helene, which caused the hurricane to turn westward on 19 September. The following day, Helene turned northward ahead of a large deep-layer trough along the East Coast. Moderate southwesterly shear ahead of this trough induced additional weakening, and Helene was a category 1 hurricane when it passed about 475 n mi east of Bermuda early on 21 September. Thereafter, Helene turned east-northeastward over the open waters of the central Atlantic and retained hurricane strength until it became extratropical on 24 September about 275 n mi northwest of the Azores.

On 25 and 26 September, the extratropical cyclone moved northeastward and weakened to a gale center before passing very near the west coast of Ireland on 27 September. The system produced gale-force wind gusts across much of Ireland and northwestern Scotland on 27–28 September. A wind gust of 49 kt was reported at the Valentia Observatory on the southwestern coast of Ireland, and in Scotland a wind gust of 64 kt was reported on South Uist Island in the Outer Hebrides. Just before reaching northwestern Scotland, the extratropical remnant of Helene merged with a larger extratropical low on 28 September.

The strongest winds measured in Helene were from a NOAA reconnaissance aircraft, which reported 111 kt at a flight level of 850 mb in the eastern eyewall at 1831

UTC 17 September. The standard adjustment ratio for this flight level (Franklin et al. 2003) yields a surface wind of 89 kt, which was in good agreement with an SFMR maximum wind of 88 kt on this flight. QuikSCAT data on 22–23 September were particularly helpful in establishing Helene's status as a hurricane until its extratropical transition on 24 September. A few hours before Helene became extratropical it passed within about 20 n mi of drifting buoy 44613 (located at 40.3°N, 39.6°W), which reported a minimum pressure of 971.8 mb at 0900 UTC 24 September.

j. Hurricane Isaac, 27 September–2 October

Isaac developed from a tropical wave that crossed the west coast of Africa on 18 September. Disturbed weather associated with the wave began to show signs of organization about 900 n mi west of the Cape Verde Islands on 23 September, when Dvorak classifications were initiated. As the large disturbance moved west-northwestward over the next few days, convection was intermittent under the influence of moderate to strong upper-level winds. By 27 September the upper-level winds had relaxed, and the system developed into a tropical depression about 810 n mi east-southeast of Bermuda.

The depression strengthened to a tropical storm early the next day, although the cyclone was slow to strengthen further as it moved over cool waters upwelled by Hurricanes Gordon and Helene. In addition, mid- to upper-level dry air had become entrained into Isaac's core and the cyclone took on a subtropical appearance on 28 September, with little convection near the core. Initially, Isaac moved northwestward around an upper-level low to its west-southwest, but on 29 September the cyclone turned west-northwestward in response to midlevel ridging over the central Atlantic, away from the upwelled waters and into an environment of lower shear. Deep convection redeveloped near the center, the cloud pattern became more consolidated, and Isaac began to strengthen, becoming a hurricane near 1200 UTC 30 September. Isaac reached its peak intensity of 75 kt around 0000 UTC 1 October, while centered about 285 n mi east of Bermuda.

Later that day, Isaac began to recurve around the western periphery of the subtropical ridge with an increase in forward speed, moving quickly to the north-northeast the next day ahead of an approaching deep-layer trough. During this time, Isaac encountered increasing southwesterly shear and cooler waters. By 1200 UTC 2 October, it weakened to a tropical storm. While racing toward the northeast at around 35 kt, Isaac's center passed about 35 n mi southeast of the Avalon Peninsula of Newfoundland late in the afternoon. Tropical storm–force winds were felt across portions of the southern Avalon Peninsula; at Cape Race sustained winds reached 40 kt and gusts reached 52 kt. Reported rainfall amounts were generally less than 25 mm. As it passed Newfoundland, Isaac maintained a core of strong winds and convection near the center, but it lost tropical characteristics quickly thereafter. By 0000 UTC 3 October Isaac had become extratropical, and it was absorbed within a larger extratropical low by 1800 UTC that day.

There were no reports of damage or casualties associated with Isaac.

3. Forecast verifications and warnings

For all operationally designated tropical (or subtropical) cyclones in the Atlantic and eastern North Pacific basins, the NHC issues an official forecast of the cyclone's center position and maximum 1-min surface wind speed. Forecasts are issued every 6 h and contain projections valid at 12, 24, 36, 48, 72, 96, and 120 h after the forecast's nominal initial time (0000, 0600, 1200, or 1800 UTC). At the conclusion of the season, forecasts are evaluated by comparing the projected positions and intensities to the corresponding poststorm derived "best track" positions and intensities for each cyclone. A forecast is included in the verification only if the system is classified in the best track as a tropical (or subtropical) cyclone at both the forecast's initial time and at the projection's valid time. All other stages of development (e.g., tropical wave, remnant low, extratropical) are excluded. For verification purposes, forecasts associated with special advisories[3] do not supersede the original forecast issued for that synoptic time; rather, the original forecast is retained. All verifications reported here include the depression stage.

It is important to distinguish between *forecast error* and *forecast skill*. Track forecast error is defined as the great-circle distance between a cyclone's forecast position and the best-track position at the forecast verification time. Skill, on the other hand, represents a normalization of forecast error against some standard or baseline. By convention, tropical cyclone forecast skill is positive when forecast errors are smaller than the errors from the baseline. Particularly useful skill standards are independent of operations (and hence can be

[3] Special advisories are issued whenever an unexpected significant change has occurred or when U.S. watches or warnings are to be issued between regularly scheduled advisories. The treatment of special advisories in forecast databases has not been consistent over the years. The current practice of retaining and verifying the original advisory forecast began in 2005.

TABLE 6. Homogenous comparison of official and CLIPER5 track forecast errors in the Atlantic basin for the 2006 season for all tropical and subtropical cyclones. Long-term averages are shown for comparison.

	Forecast period (h)						
	12	24	36	48	72	96	120
2006 mean official error (n mi)	29.7	50.8	71.9	97.0	148.7	205.5	265.3
2006 mean CLIPER5 error (n mi)	43.4	90.0	144.6	203.3	299.1	331.6	333.7
2006 mean official skill relative to CLIPER5 (%)	32	44	50	52	50	38	21
2006 mean official bias vector [° (n mi)$^{-1}$]	314/5	310/9	319/14	335/19	352/28	311/17	257/82
2006 No. of cases	223	205	187	169	132	100	78
2001–05 mean official error (n mi)	37.3	64.5	91.3	118.3	171.4	231.1	303.3
2001–05 mean CLIPER5 error (n mi)	49.8	103.9	164.7	222.0	327.7	441.9	548.1
2001–05 mean official skill relative to CLIPER5 (%)	25	38	45	47	48	48	45
2001–05 mean official bias vector [° (n mi)$^{-1}$]	305/6	315/13	320/21	322/27	310/24	344/19	034/36
2001–05 No. of cases	1930	1743	1569	1410	1138	913	742
2006 official error relative to 2001–05 mean (%)	−20	−21	−21	−18	−13	−11	−13
2006 CLIPER5 error relative to 2001–05 mean (%)	−13	−13	−12	−8	−9	−25	−39

applied retrospectively to historical data), and provide a measure of inherent forecast difficulty. For tropical cyclone track forecasts, the skill baseline is the Climatology and Persistence (CLIPER5) model, which contains no information about the current state of the atmosphere (Neumann 1972; Aberson 1998). The version of CLIPER5 presently in use is based on developmental data from 1931 to 2004 for the Atlantic and from 1949 to 2004 for the eastern Pacific.

Table 6 presents the results of the NHC official track forecast verification for the 2006 season, along with results averaged for the previous 5-yr period of 2001–2005.[4] Mean track errors ranged from 30 n mi at 12 h to 265 n mi at 120 h. It is seen that mean official track forecast errors were smaller in 2006 than during the previous 5-yr period (by roughly 15%–20% out to 72 h), and at forecast projections through 72 h the errors established new all-time lows. Since 1990, 24–72-h official track forecast errors have been reduced by roughly 50% (Franklin 2007). Fairly substantial vector biases at the longer ranges were noted in 2006; at 120 h the official forecast bias was 82 n mi to the west of the verifying position. This bias, about 35% of the mean error magnitude, was about twice as large as the average bias in the leading dynamical track models, and was most pronounced for storms south of 20°N, suggesting a tendency to inadequately consider forecast guidance calling for recurvature.

While the track forecasts at each time period were more accurate in 2006 than they had been over the previous 5-yr period, only the forecasts from 12–72 h were also more skillful. The improved skill at 12–72 h in 2006 occurred despite the fact that CLIPER5 errors during 2006 were also below average, indicating below-average forecast difficulty. It is worth noting that the 96- and 120-h CLIPER5 errors and sample sizes were anomalously low in 2006, so the loss of skill at these time periods is likely of no long-term significance. An examination of annual skill trends (not shown) suggests that shorter-range forecast skill continues to increase, while no clear trend is apparent for 72 h and beyond.

Forecast intensity error is defined as the absolute value of the difference between the forecast and best-track intensity at the forecast verifying time. The skill of intensity forecasts is assessed using a modified version of the Statistical Hurricane Intensity Forecast (SHIFOR5) climatology and persistence model (Jarvinen and Neumann 1979; Knaff et al. 2003). The modified model, known as DSHIFOR5, is constructed by taking the output from SHIFOR5 and applying the decay rate of DeMaria et al. (2006). The application of the decay component requires a forecast track, which here is given by CLIPER5. The use of DSHIFOR5 as the intensity skill benchmark is new for 2006. On average, DSHIFOR5 errors are about 5%–15% lower than SHIFOR5 in the Atlantic basin from 12 to 72 h, and about the same as SHIFOR5 at 96 and 120 h.

Table 7 presents the results of the NHC official intensity forecast verification for the 2006 season, along with results for the preceding 5-yr period. Mean forecast errors in 2006 were very close to the 5-yr means, with errors ranging from about 7 kt at 12 h to just below 20 kt at 96 and 120 h. Forecast biases, however, were large and positive—near 5 kt at 72 h and over 7 kt at

[4] It has been traditional to use a 10-yr sample to establish representative NHC official forecast error characteristics. Given the increase in storm activity in recent years, as well as the significant improvements in track forecast accuracy, it is now felt that a 5-yr sample is more representative of the state of the science.

TABLE 7. Homogenous comparison of official and DSHIFOR5 intensity forecast errors in the Atlantic basin for the 2006 season for all tropical and subtropical cyclones. Long-term averages are shown for comparison.

	Forecast period (h)						
	12	24	36	48	72	96	120
2006 mean official error (kt)	6.5	10.0	12.4	14.3	18.1	19.6	19.0
2006 mean DSHIFOR5 error (kt)	6.7	9.3	11.4	12.9	13.8	14.4	13.1
2006 mean official skill relative to DSHIFOR5 (%)	3	−8	−9	−11	−31	−36	−45
2006 official bias (kt)	0.7	2.2	2.7	3.4	5.0	7.3	6.1
2006 No. of cases	223	205	187	169	132	100	78
2001–05 mean official error (kt)	6.3	9.8	12.1	14.3	18.4	19.8	21.8
2001–05 mean DSHIFOR5 error (kt)	7.8	11.7	15.0	18.1	22.1	24.8	25.5
2001–05 mean official skill relative to DSHIFOR5 (%)	19	16	19	21	17	20	15
2001–05 official bias (kt)	0.2	0.3	0.1	−0.4	−0.7	−1.8	−1.6
2001–05 No. of cases	1930	1743	1569	1410	1138	913	742
2006 official error relative to 2001–05 mean (%)	3	2	2	0	−2	−1	−13
2006 DSHIFOR5 error relative to 2001–05 mean (%)	−14	−21	−24	−29	−38	−42	−49

96 h. In contrast, intensity biases for the period 2001–05 were near zero. It is interesting that these large positive biases occurred in a year for which there were very few instances of rapid strengthening (only 3.3% of all 24-h intensity changes qualified),[5] but which followed a season that featured many such cases (2005 featured a 7.1% occurrence rate), and indeed the 2001–05 period as a whole had numerous strong and rapidly deepening storms. The lack of such storms in 2006 led to DSHIFOR5 errors that were considerably below normal (i.e., this year's storms should have been relatively easy to forecast). However, these low DSHIFOR5 errors, coupled with the tendency to overforecast intensification, resulted in strongly negative official forecast skill in 2006.

Additional information on the 2006 forecast verification, both for official NHC forecasts and the objective guidance models, is given by Franklin (2007).

NHC defines a hurricane (or tropical storm) warning as a notice that 1-min mean winds of hurricane (or tropical storm) force are expected within a specified coastal area within the next 24 h. A watch indicates that those conditions are possible within 36 h. Table 8 lists lead times associated with those tropical cyclones that affected the United States in 2006. Because observations are generally inadequate to determine when hurricane or tropical storm conditions first reach the coastline, for purposes of this discussion, lead time is defined as the time elapsed between the issuance of the watch or warning and the time of landfall or closest approach of the center to the coastline. Such a definition will usually overstate by a few hours the actual preparedness time available, particularly for tropical storm conditions. The table includes only the most significant (i.e., strongest) landfall for each cyclone, and only verifies the strongest conditions occurring on shore. The issuance of warnings for non-U.S. territories is the responsibility of the governments affected and is not tabulated here. The table shows that warning goals were generally met in 2006, although no watch preceded the warning issued for Alberto.

[5] Following Kaplan and DeMaria (2003), rapid intensification is defined here as a 30-kt-or-greater increase in maximum winds in a 24-h period, and corresponds to the 5th percentile of all intensity changes in the Atlantic basin.

TABLE 8. Watch and warning lead times (see text) for tropical cyclones affecting the United States in 2006. For cyclones with multiple landfalls, the most significant is given. If multiple watch or warning types (TS or H) were issued, the type corresponding to the most severe conditions experienced over land is given.

Storm	Landfall or point of closest approach	Watch type: lead time (h)	Warning type: lead time (h)
Alberto	Adams Beach, FL	None issued	TS: 32
Beryl	Nantucket, MA	TS: 34	TS: 22
Ernesto	Oak Island, NC	H: 55	TS: 37

Acknowledgments. The cyclone summaries are based on tropical cyclone reports written by the authors and their NHC hurricane specialist colleagues: Lixion Avila, Jack Beven, Richard Pasch, Richard Knabb, Stacy Stewart, Eric Blake, Jamie Rhome, and Michelle Mainelli. The authors thank Chris Velden and David Stettner of the University of Wisconsin—Madison Cooperative Institute for Meteorological Satellite Studies (CIMSS) for the satellite images presented here. Tropical Prediction Center colleague Ethan Gibney produced the track chart. Additional figures were provided by Joan David and Eric Blake. Much of the local impact information contained in the individual storm summa-

ries was compiled by local NWS Weather Forecast Offices in the affected areas.

REFERENCES

Aberson, S. D., 1998: Five-day tropical cyclone track forecasts in the North Atlantic basin. *Wea. Forecasting,* **13,** 1005–1015.

——, and J. L. Franklin, 1999: Impact on hurricane track and intensity forecasts of GPS dropwindsonde observations from the first season flights of the NOAA Gulfstream-IV jet aircraft. *Bull. Amer. Meteor. Soc.,* **80,** 421–427.

Bell, G. D., E. Blake, C. W. Landsea, M. Chelliah, R. Pasch, K. C. Mo, and S. B. Goldenberg, 2007: State of the Climate in 2006—Atlantic basin. *Bull. Amer. Meteor. Soc.,* **88** (Suppl.), doi:10.1175/BAMS-88-6-StateoftheClimate.

DeMaria, M., J. A. Knaff, and J. Kaplan, 2006: On the decay of tropical cyclone winds crossing narrow landmasses. *J. Appl. Meteor.,* **45,** 491–499.

Dvorak, V. E., 1984: Tropical cyclone intensity analysis using satellite data. NOAA Tech. Rep. NESDIS 11, National Oceanic and Atmospheric Administration, Washington, DC, 47 pp.

Franklin, J. L., cited 2007: 2006 National Hurricane Center Forecast Verification Report. [Available online at http://www.nhc.noaa.gov/verification/pdfs/Verification_2006.pdf.]

——, M. L. Black, and K. Valde, 2003: GPS dropwindsonde wind profiles in hurricanes and their operational implications. *Wea. Forecasting,* **18,** 32–44.

Hart, R. E., 2003: A cyclone phase space derived from thermal wind and thermal asymmetry. *Mon. Wea. Rev.,* **131,** 585–616.

Hawkins, J. D., T. F. Lee, J. Turk, C. Sampson, F. J. Kent, and K. Richardson, 2001: Real-time Internet distribution of satellite products for tropical cyclone reconnaissance. *Bull. Amer. Meteor. Soc.,* **82,** 567–578.

Hebert, P. J., and K. O. Poteat, 1975: A satellite classification technique for subtropical cyclones. NOAA Tech. Memo. NWS SR-83, 25 pp. [Available from National Weather Service, Fort Worth, TX 76102.]

Herndon, D. C., and C. Velden, 2004: Upgrades to the UW-CIMSS AMSU-based tropical cyclone intensity estimation algorithm. Preprints, *26th Conf. on Hurricane and Tropical Meteorology,* Miami, FL, Amer. Meteor. Soc., 118–119.

Hock, T. F., and J. L. Franklin, 1999: The NCAR GPS dropwindsonde. *Bull. Amer. Meteor. Soc.,* **80,** 407–420.

Jarvinen, B. R., and C. J. Neumann, 1979: Statistical forecasts of tropical cyclone intensity for the North Atlantic basin. NOAA Tech. Memo. NWS NHC-10, 22 pp.

Kaplan, J., and M. DeMaria, 2003: Large-scale characteristics of rapidly intensifying tropical cyclones in the North Atlantic basin. *Wea. Forecasting,* **18,** 1093–1108.

Kistler, R., and Coauthors, 2001: The NCEP–NCAR 50-Year Reanalysis: Monthly means CD-ROM and documentation. *Bull. Amer. Meteor. Soc.,* **82,** 247–267.

Knaff, J. A., M. DeMaria, B. Sampson, and J. M. Gross, 2003: Statistical, five-day tropical cyclone intensity forecasts derived from climatology and persistence. *Wea. Forecasting,* **18,** 80–92.

Neumann, C. B., 1972: An alternate to the HURRAN (hurricane analog) tropical cyclone forecast system. NOAA Tech. Memo. NWS SR-62, 24 pp.

Saffir, H. S., 1973: Hurricane wind and storm surge. *Mil. Eng.,* **423,** 4–5.

Simpson, R. H., 1974: The hurricane disaster potential scale. *Weatherwise,* **27,** 169, 186.

Tsai, W.-Y., M. Spender, C. Wu, C. Winn, and K. Kellogg, 2000: SeaWinds of QuikSCAT: Sensor description and mission overview. *Proc. Int. Geoscience and Remote Sensing Symp.,* Vol 3., Honolulu, HI, IEEE, 1021–1023.

Uhlhorn, E. W., and P. G. Black, 2003: Verification of remotely sensed sea surface winds in hurricanes. *J. Atmos. Oceanic Technol.,* **20,** 99–116.

Velden, C. S., and K. F. Brueske, 1999: Tropical cyclone warm cores as observed from the NOAA polar orbiting satellite's new Advanced Microwave Sounder Unit. Preprints, *23rd Conf. on Hurricane and Tropical Meteorology,* Dallas, TX, Amer. Meteor. Soc., 182–185.